

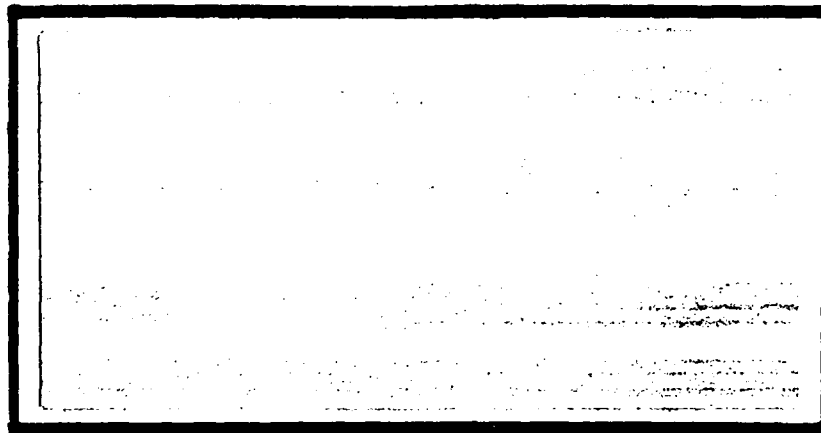
DTIC FILE COPY

1

AD-A216 244



S DTIC
 ELECTE
 JAN 0 2 1990
 B **D**



DEPARTMENT OF THE AIR FORCE
 AIR UNIVERSITY
AIR FORCE INSTITUTE OF TECHNOLOGY

Wright-Patterson Air Force Base, Ohio

DISTRIBUTION STATEMENT A

Approved for public release;
 Distribution Unlimited

89 12 29 050

①

AFIT/GA/ENY/89D-5

A FRACTIONAL CALCULUS MODEL
OF AEROELASTICITY
THESIS

David V. Swinney
Captain, USAF

AFIT/GA/ENY/89D-5

Approved for public release; distribution unlimited

DTIC
ELECTE
JAN 0 2 1990
S B D

AFIT/GA/ENY/89D-5

A FRACTIONAL CALCULUS MODEL
OF AEROELASTICITY

THESIS

Presented to the Faculty of the School of Engineering
of the Air Force Institute of Technology

Air University

In Partial Fulfillment of the
Requirements for the Degree of
Master of Science in Astronautical Engineering

David V. Swinney, B.S.

Captain, USAF

December 1989

Approved for public release; distribution unlimited

Preface

My objective in writing this thesis was to employ fractional order time derivatives to build a new model of aeroelastic behavior. My approach allows an intuitive and direct solution to the equations of aeroelastic instability. I have restricted my development to an airfoil section in freestream flow, so it should provide a solid base for more complex models incorporating additional equations for three dimensional effects.

I wish to express my heartfelt thanks to LtCol Ronald Bagley. Without his guidance and encouragement I could not have begun this work.

I would also like to thank Ted Fecke and the propulsion lab for their support and interest in this basic development. A word of thanks to the flight dynamics lab as well for providing me with some insight regarding current applications of aeroelastic modeling.



Accession For	
NTIS GRA&I	<input checked="" type="checkbox"/>
DTIC TAB	<input type="checkbox"/>
Unannounced	<input type="checkbox"/>
Justification	
By _____	
Distribution/	
Availability Codes	
Dist	Avail and/or Special
A-1	

Table of Contents

Preface.....	ii
List of Figures	iv
List of Symbols	v
Abstract.....	vii
I. Introduction	1
Aeroelasticity	1
Fractional Calculus	3
II. Models	4
Theodorsen's Function	4
Experimental Data	14
III. Time Domain Functions	20
Wagner's Function	21
Küssner's Function	23
IV. Flutter Prediction	25
Fractional Approach	28
Comparison With Existing Methods	34
VI. Summary and Conclusions	37
Appendix A: Complex Pressure Coefficient Data	39
Appendix B: Fractional Order State Equation	45
Appendix C: MATLAB Matrix Construction and Solution	47
Bibliography	48
Vita.....	50

List of Figures

Theodorsen Function vs NASTRAN Model	6
Theodorsen Function vs Padé Model	7
Theodorsen Function vs Fractional Calculus Model	8
Generalized Theodorsen Function	
Edwards (7:22)	11
NASTRAN Model	12
Fractional Calculus Model	13
Complex Pressure at 3.3% chord	16
Variation in Phase Lag	17
Lift Coefficient Variation	18
Wagner's Function	23
Typical Section Geometry	25
$s^{1/6}$ plane eigenvalues	32
s plane eigenvalues	33
Root Locus	
Edwards (7:51)	35
Fractional Method	36

List of Symbols

a	Displacement of elastic axis from airfoil center (nondimensionalized by b)
b	Semichord of a typical airfoil section
$C(\bar{s})$	Theodorsen's Function
$\hat{C}(\bar{s})$	Fractional Calculus Model of Theodorsen's Function
C_l	Lift coefficient
C_p	Pressure coefficient
d	Phase shift contribution parameter
$E_\beta(x)$	Mittag-Leffler Function of order β
F	Constant defined in equation (4)
g	Structural damping factor
h	Plunge coordinate nondimensionalized by b
$I_n(\bar{s})$	Modified Bessel Function of the First Kind of Order n
i	square root of -1
$K_n(\bar{s})$	Modified Bessel Function of the Third Kind of Order n
[K]	Pseudostiffness matrix
k	Reduced (dimensionless) frequency $\omega b/U$
$k_1(\sigma)$	Wagner's Function
$k_2(\sigma)$	Küssner's Function
$L\{x\}$	Laplace Transform of $\{x\}$
$L^{-1}\{x\}$	Inverse Laplace Transform of $\{x\}$
[M]	Pseudomass matrix
m_s	Airfoil section mass
n	Index of summation
r_α	Airfoil section radius of gyration
s	Laplace transform variable
\bar{s}	Dimensionless Laplace transform variable
t	Time

U	Freestream velocity of the airfoil
$\{x_s\}$	Laplace transform of a coordinate vector
$\{X\}$	Fractional derivative state vector
x_α	Distance from mass center to elastic axis nondimensionalized by b
α	Airfoil section angle of incidence
β	Constant defined in equation (4)
$\Gamma(x)$	Gamma Function
ρ	Freestream density
σ	Dimensionless time (tU/b)
μ	Mass ratio ($m_s/\pi\rho b^2$)
ω	Oscillation frequency of airfoil
ω_α	Torsion mode natural frequency
ω_h	Plunge mode natural frequency

Abstract

This thesis introduces a new model of aeroelastic behavior. It simplifies the unsteady aerodynamic force expressions by employing fractional order time derivatives to create a compact fractional order polynomial that models unsteady aerodynamic forces in the transform domain.

To solve the flutter and divergence problems, the equations of motion for a typical section are expressed in fractional form. The resulting structural and aerodynamic equations of motion can be combined into a single fractional derivative eigenvalue problem. This approach allows a solution to the stability of a lifting surface which obtains the system eigenvalues directly rather than relying on a separately defined stability parameter.

I. Introduction

The purpose of this study was to develop a closed form approximate solution to the aeroelastic instability problem. While the intended application is in turbine blade instability, this study develops a basic model not limited to internal flow. The concepts presented are equally applicable to typical section approaches to wing instability and can be generalized to treat airfoils with control surfaces.

Aeroelasticity

The typical section model of an airfoil has a long history of use by aeroelasticians. Most methods of determining airfoil flutter characteristics have their roots in the typical section model. Early work by Theodorsen and others provided an exact solution for the two-dimensional flow of an incompressible fluid around an infinitely thin flat plate with a wake composed of a plane vortex sheet (smooth trailing edge flow) (17:6-7).

Theodorsen went on to develop a transcendental function which describes the variation in lift due to circulation resulting from the simple harmonic motion of an oscillating plate. Theodorsen's function describes the reduction and phase shift of lift with increasing "reduced frequency" ($k = \omega b/U$ or actual frequency multiplied by the semi-chord and divided by the freestream velocity). The difficulty with this approach is that, since Theodorsen's

function is difficult to pose as a time domain operator, it has typically been applied only to aerodynamic forces resulting from pure sinusoidal motion. This has helped various "indirect" methods to retain their popularity (6:106).

Indirect approaches to the aeroelasticity problem rely on the creation of a "stability boundary", with instability presumed to occur when one of the limits of such a boundary is exceeded. While such methods provide good estimates of critical flutter speeds, it is difficult to interpret their results in terms of stability margins. Since these methods rely on the disappearance of a neutral stability solution, they cannot give precise information about the actual behavior of a system away from its critical points (3:564-568), (4:235).

One such approach to finding critical flutter speeds is the "U-g" method. It employs an artificial structural damping factor, g , which is allowed to vary with airspeed. The "stability boundary" for this method is $g \leq 0$; when g is negative, the structure "adds" energy to reach a neutrally stable condition. The system becomes unstable when a positive g would be needed to produce a neutral stability solution (3:561-568).

A more straightforward approach of solving for the eigenvalues of the system has received more attention in recent years. The eigenvalue solution provides a natural stability limit at the imaginary axis, a simple solution to the instability (flutter or divergence) speeds, and a good measure of the degree of stability at a given speed.

Fractional Calculus

The power previously demonstrated by the fractional calculus in modeling frequency dependent properties and describing linear phenomena (2:741-742) indicated that a fractional calculus based model might produce an accurate approximation to the reduction in lift and shift in phase angle following airfoil movement modeled by Theodorsen's function. Existing approximations to Theodorsen's function, such as the Padé polynomial and R. T. Jones approximations (8:215,344), (11:31-38), (16:6,7) use integer power polynomials which are the Laplace transforms of exponential functions and their integer derivatives. The fractional derivative, as defined in equation (1), has a Laplace domain transformation which yields a fractional power of the Laplace variable corresponding to the order of the derivative as shown in equation (2).

$$D^{\alpha}\langle x(t) \rangle = \frac{1}{\Gamma(1-\alpha)} \frac{d}{dt} \int_0^t \frac{x(\tau)}{(t-\tau)^{\alpha}} d\tau \quad (1)$$

$$L\{D^{\alpha}\langle x(t) \rangle\} = s^{\alpha}L\{x(t)\} \quad (2)$$

A fractional calculus based "generalized polynomial" would contain fractional powers of the Laplace variable. Such a polynomial would be a Laplace transform of a generalized exponential function.

The model based on this concept and presented in this work has the advantages of accurate modeling of Theodorsen's function in a very compact form, consistent time-domain representations of lift, and a direct eigenvalue solution.

II. Models

The first step in development of a fractional derivative model of aeroelasticity is the accurate modeling of the Theodorsen function. The Theodorsen's function model can then be used to develop the time domain responses of the system. The common aeroelastic functions which describe such time responses are Wagner's and Küssner's functions.

Theodorsen's Function

Theodorsen's function is a transcendental function of reduced frequency ($k = \omega b/U$) and is an exact expression used to construct the circulatory aerodynamic forces resulting from the harmonic oscillation of a flat plate in an incompressible flow (8:212-215). Various expressions are available depending on the desired argument. Equation (3) is an exact expression of the Theodorsen function on the imaginary axis. (This function will operate throughout the complex plane if ik is replaced by a complex variable, \bar{s} .)

$$C(ik) = K_1(ik)/[K_0(ik)+K_1(ik)] \quad (3)$$

$K_n(ik)$ is a modified Bessel function of the third kind of order n with an argument on the imaginary axis. The real part of the Theodorsen function varies from 1.0 to 0.5 as its argument varies from zero to infinity, so modeling this function using a polynomial requires that the ratio of coefficients of the lowest order term must be 1.0 while the ratio of coefficients of the highest order term must be 0.5. Adding parameters to improve the fit of integer power

polynomials means adding higher powers of the argument. By introducing a fractional power as a parameter, the function fit may be manipulated by reducing the order of the polynomial to a fractional value as shown in equation (4).

$$\hat{C}(\bar{s}) = (1 + F\bar{s}^\beta)/(1 + 2F\bar{s}^\beta) \quad (4)$$

Optimizations of a fractional order polynomial model of the Theodorsen function over several decades of reduced frequency result in a fractional exponent near 0.82. Since the optimum is not too sensitive to this exponent, a rational exponent of $\beta = 5/6$ was chosen to simplify the treatment of the resulting equations. The fractional term coefficient F was then optimized for a wide frequency range resulting in a value of $F = 2.19$. The fractional calculus model shown in equation (4) will be shown to have good accuracy over all reduced frequencies and a wide range of complex arguments.

Figures 1 through 3 show the relative accuracy of various approximations to the Theodorsen function. The accuracy of fit is compared to the Theodorsen's real and imaginary parts over four decades of reduced frequency using a root mean square error measure.

Figure 1 shows the Theodorsen function compared with the polynomial model developed by R.T. Jones and used by the aeroelasticity module of NASTRAN (16:7) given in equation (5). The root mean square error for this model is 0.047.

$$C(\bar{s}) \approx \sum_{n=0}^N \frac{b_n}{1 + \beta_n/\bar{s}} \quad \begin{array}{l} n = 0 \quad 1 \quad 2 \\ b_n = 1 \quad -.165 \quad -.335 \\ \beta_n = 0 \quad .0455 \quad .300 \end{array} \quad (5)$$

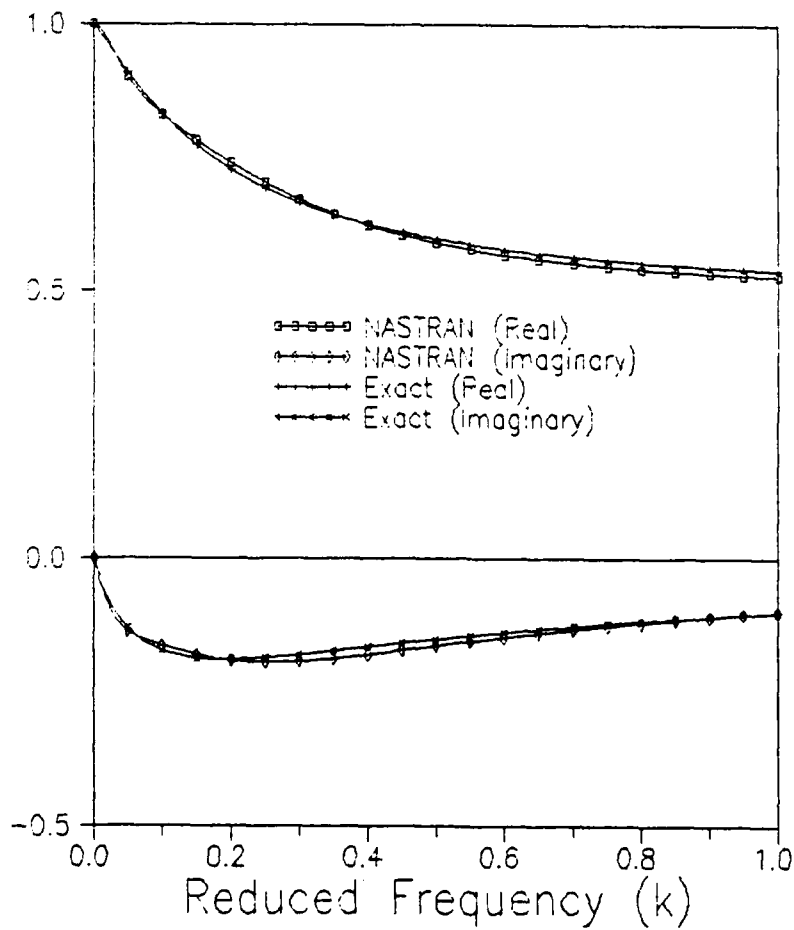


Figure 1. Theodorsen Function vs NASTRAN Model

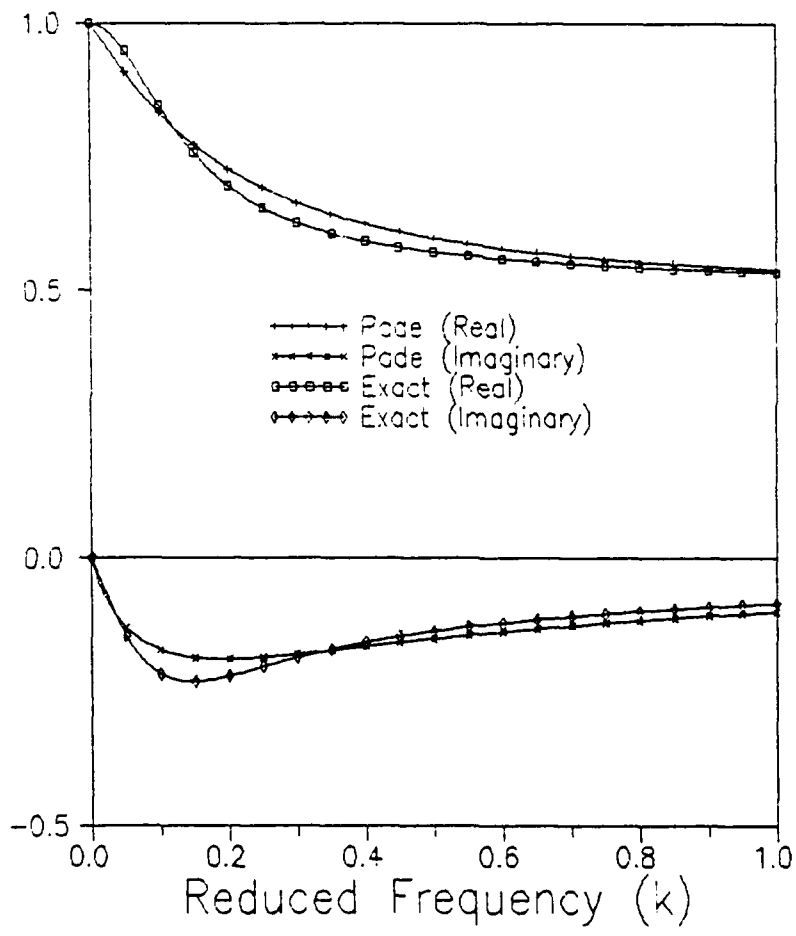


Figure 2. Theodorsen Function vs Padé Model

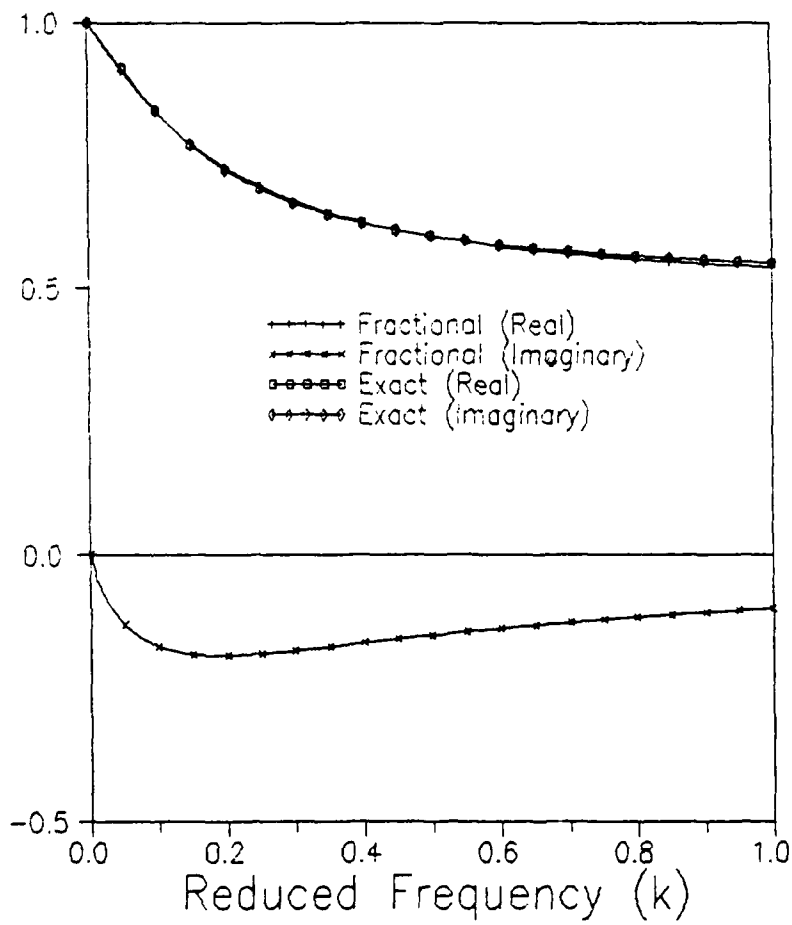


Figure 3. Theodorsen Function vs Fractional Calculus Model

Figure 2 shows the Theodorsen function vs a third order Padé Polynomial Model given by equation (6). The root mean square error for this model is 0.134.

$$C(\bar{s}) \approx \frac{(\bar{s})^3 + 3.5(\bar{s})^2 + 2.7125(\bar{s}) + .46875}{2(\bar{s})^3 + 6.5(\bar{s})^2 + 4.25(\bar{s}) + .46875} \quad (6)$$

Figure 3 shows the Theodorsen function compared with the fractional calculus model given by equation (4). The root mean square error for this model is 0.031.

In addition to providing an accurate model of the function for a wide range of imaginary frequencies, the model should be accurate for complex arguments. Since Theodorsen's function is composed of transcendental functions (Bessel or Hankel functions) it has typically been approximated by truncated series expansions or rational polynomials. Many of the approximations for these functions are useful only over a limited range of arguments or cannot be used for complex arguments.

Early work by Luke and Dengler (14:478-483) attempted to expand Theodorsen's function to treat the generalized oscillations associated with complex arguments. While the tables they generated were submitted without proof and were rejected in a series of papers (18:209), (13:212), (12:213) much of their work was useful. They introduced the use of R.T. Jones' approximation as a model of the generalized Theodorsen's function. Recent work by Edwards (7:18-24) has provided a rigorous proof of the existence of a generalized Theodorsen's function in the form of equation (7) and shown

that generalized aerodynamic loads resulting from arbitrary airfoil motions can be adequately treated using this function.

$$C(\bar{s}) = K_1(\bar{s})/[K_0(\bar{s})+K_1(\bar{s})] \quad (7)$$

$K_n(\bar{s})$ is a modified Bessel function of the third kind of order n with a complex argument. This indicates that an approximation to Theodorsen's function should be able to treat fully complex, rather than only imaginary, arguments over a wide range of reduced frequency. This will allow treatment of the stable behavior of an airfoil as well as divergence and flutter predictions.

Since the generalized Theodorsen function operates throughout the complex plane, it is more difficult to approximate than the function restricted to the imaginary axis. Figure 4 shows the generalized Theodorsen function $C(\bar{s}) = F(\bar{s}) - iG(\bar{s})$ of argument $\bar{s} = re^{i\theta}$ for several values of θ as calculated by Edwards (7:22). Figure 5 shows the generalized Theodorsen function calculated using the NASTRAN model. Note that the NASTRAN approximation loses accuracy as it approaches the negative real axis where its poles occur. The imaginary portion actually collapses back to zero when the argument lies on the negative real axis. Figure 6 shows the generalized Theodorsen function calculated using the fractional calculus model.

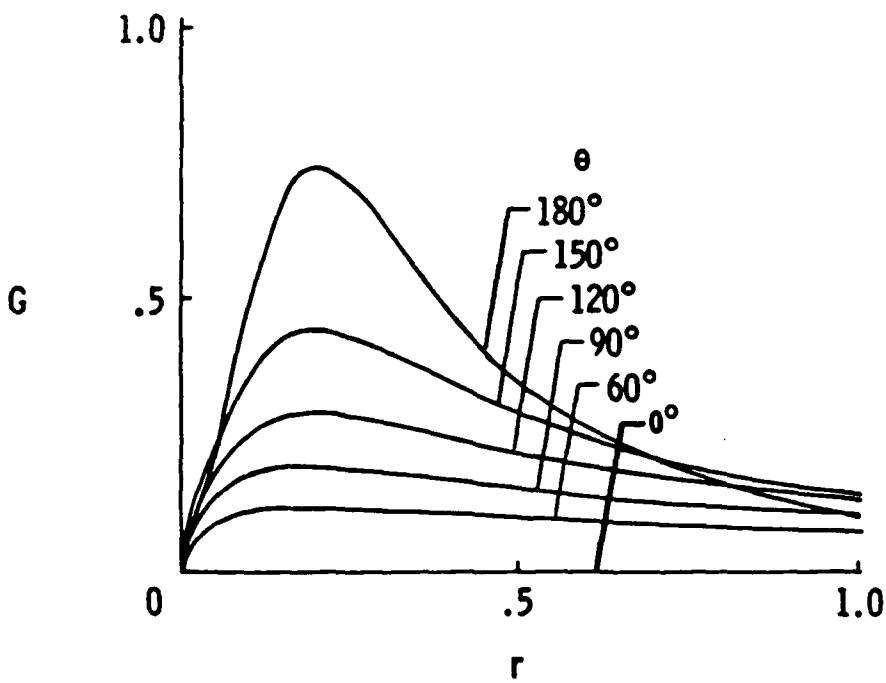
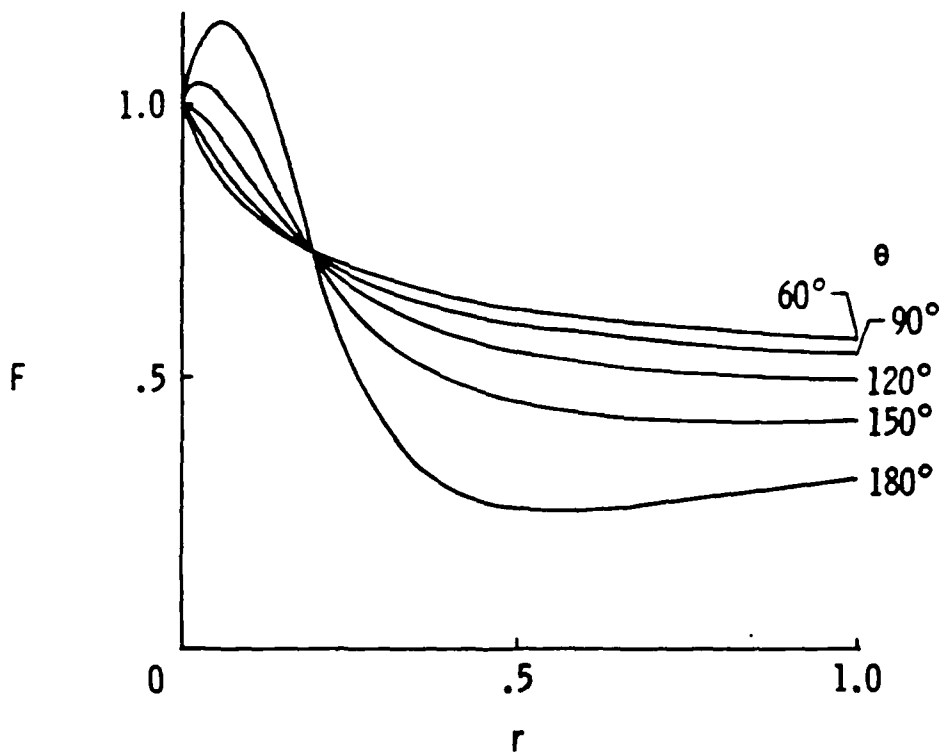


Figure 4. Generalized Theodorsen Function
Edwards (7:22)

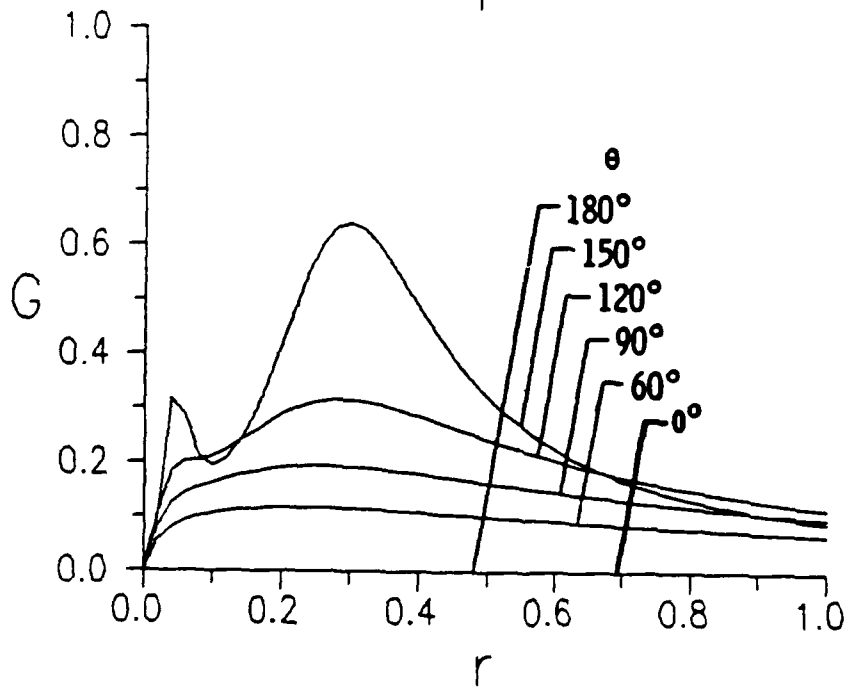
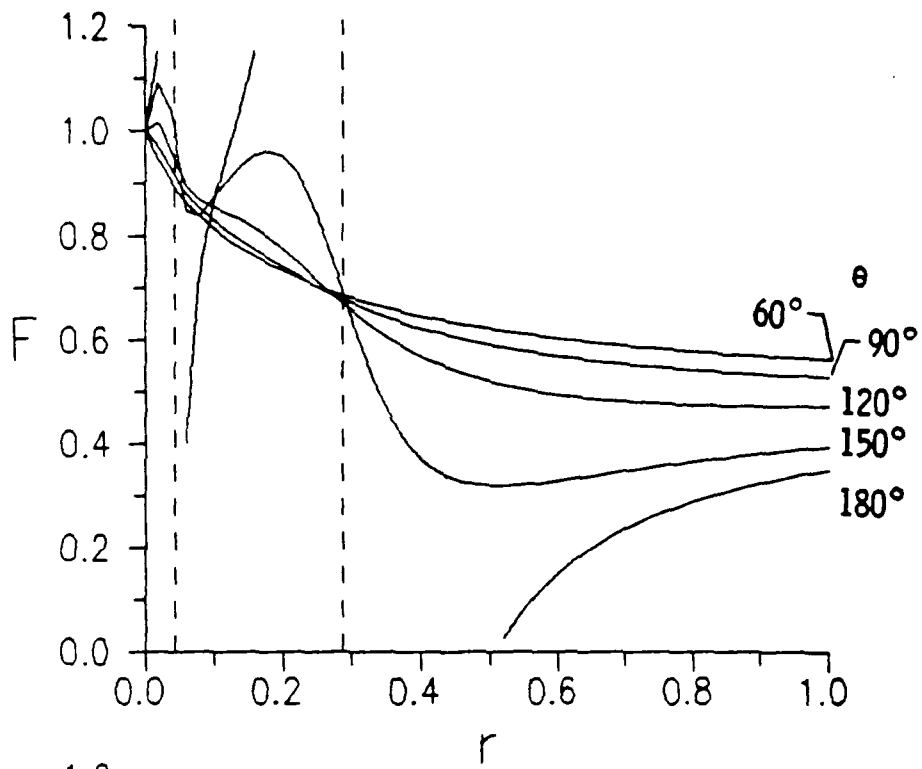


Figure 5. Generalized Theodorsen Function
NASTRAN Model

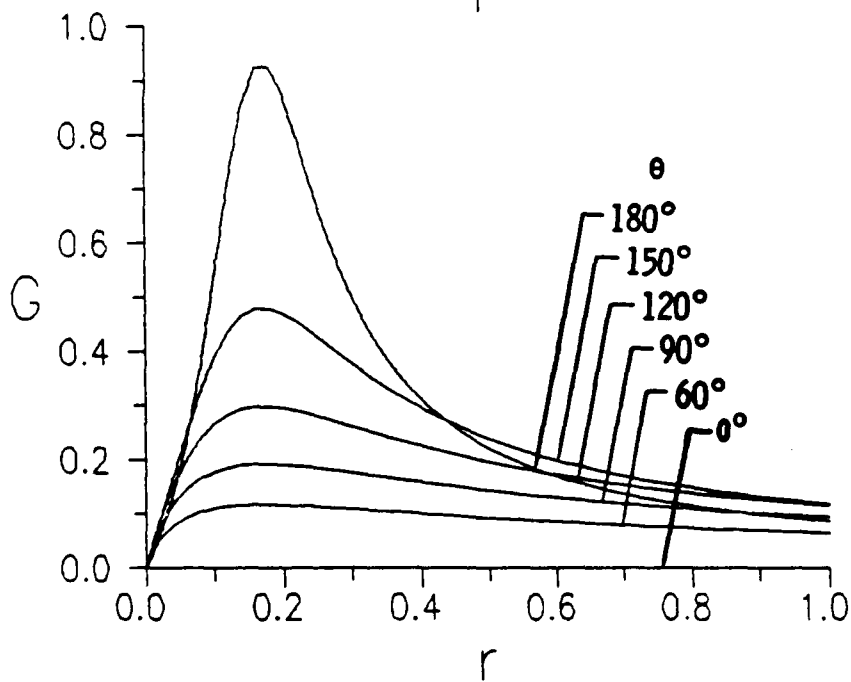
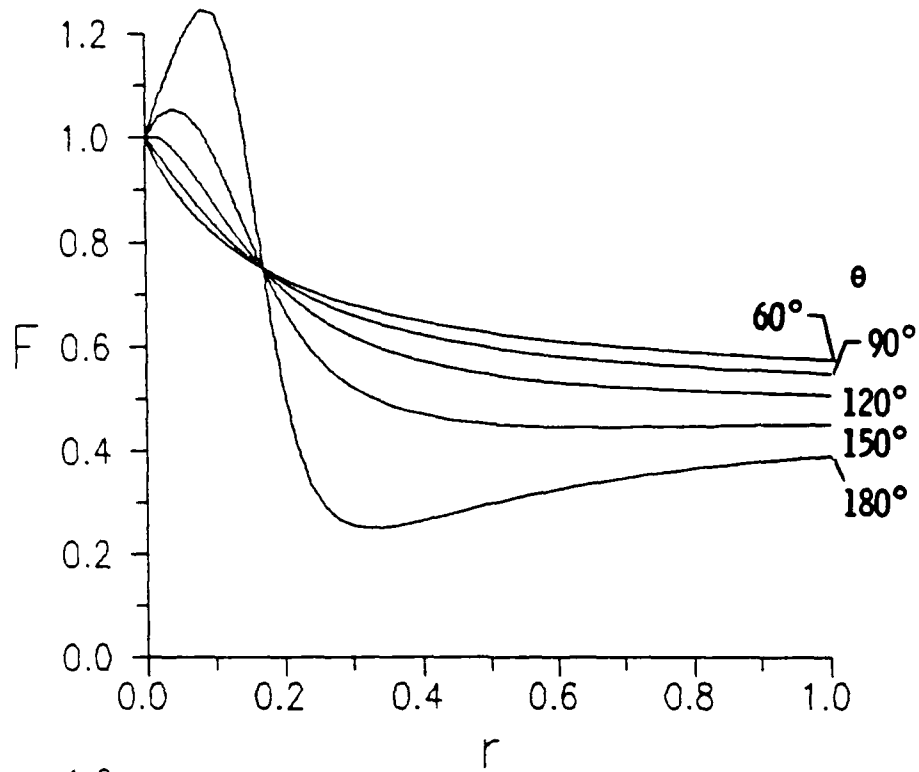


Figure 6. Generalized Theodorsen Function
Fractional Calculus Model

For complex arguments near the negative real axis, the fractional calculus model is an excellent approximation of Theodorsen's function. The fractional calculus model follows the trends of Edwards' values throughout the complex plane. Even in the areas approaching the negative real axis, however, the fractional calculus model is more accurate than other representations. Other models have negative real poles in the primary Laplace plane which cause more distortion near the negative real axis. This overall accuracy allows the fractional calculus model to simultaneously predict the critical speed at which an airfoil begins either unbounded oscillations (flutter) or a monotonic increase in position (divergence).

Given that a model of Theodorsen's function is sufficiently accurate, it should be possible to model the forces arising from an unsteady flow. The next step in modeling Theodorsen's function is to compare the model to existing data.

Experimental Data

The forces on an airfoil oscillating harmonically in a steady flow are described by the Theodorsen function. NASA Ames has published an extensive set of experimental data for oscillating airfoils in subsonic flow. The data in this section represent a 64A010 airfoil oscillating in pitch in a high Reynolds number subsonic flow (5:40).

The fundamental frequency component of the varying dynamic pressure at each point along a thin airfoil can be

interpreted as a complex number which indicates its magnitude and phase shift with respect to an input motion (5:11). This complex pressure can be modeled using Theodorsen's function. The magnitude of the contribution of each point to the overall lift coefficient varies along the airfoil, but the pressure at each location can be modeled using a fractional calculus form of Theodorsen's function plus a scaled contribution to phase lag as shown in equation (8). The scaling factors A and d vary with chord location (x).

$$C_p = A(x)C(ik) + d(x)(ik) \quad (8)$$

Figure 7 shows the variation in frequency dependent pressure coefficient at a typical chord location ($x=.033c$). Figure 8 shows the variation of the phase lag scaling factor, d, along the airfoil chord. Other pressure coefficient plots for other chord positions are given in Appendix A.

The theoretical expression for the lift coefficient, equation (9) (17:12), depends on the Theodorsen function and varies with reduced frequency.

$$C_l = A[C(ik) + 0.5ik] \quad (9)$$

This form should result from the integration of the pressure coefficients over the entire airfoil. Equation (9) indicates that the net contribution of the phase lag scaling factor to the overall lift coefficient should be 0.5. Figure 9 shows the actual data from the NASA test compared to a fractional calculus model of equation (9).

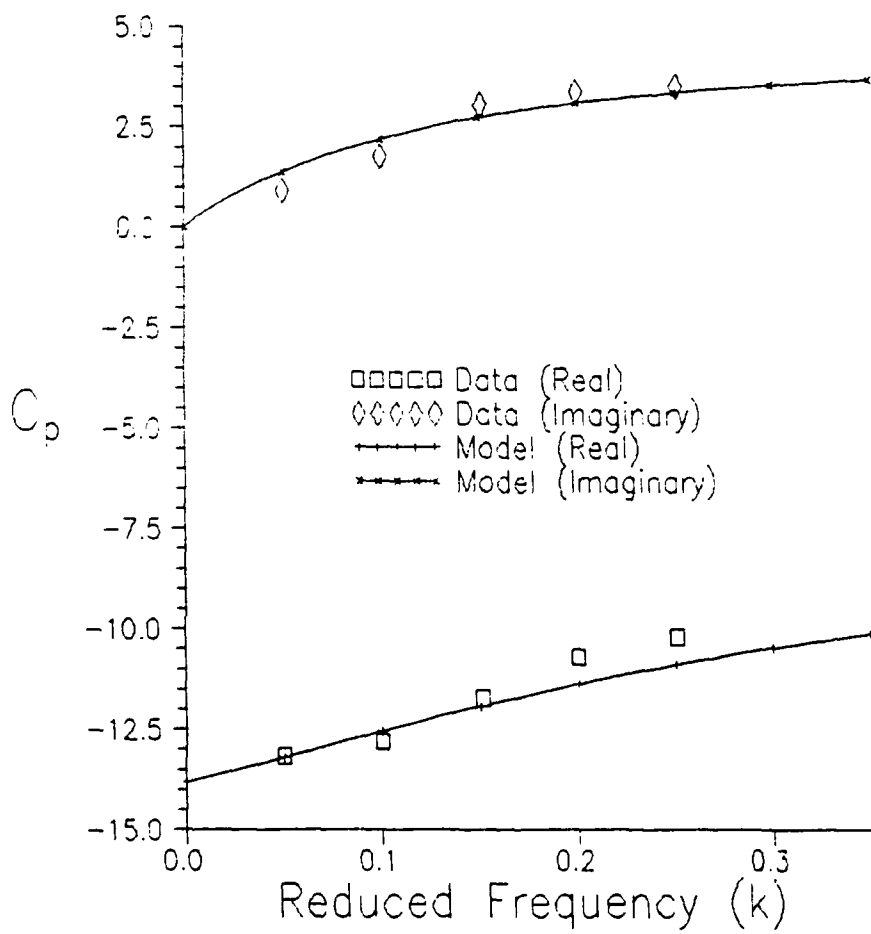


Figure 7. Complex Pressure at 3.3% chord

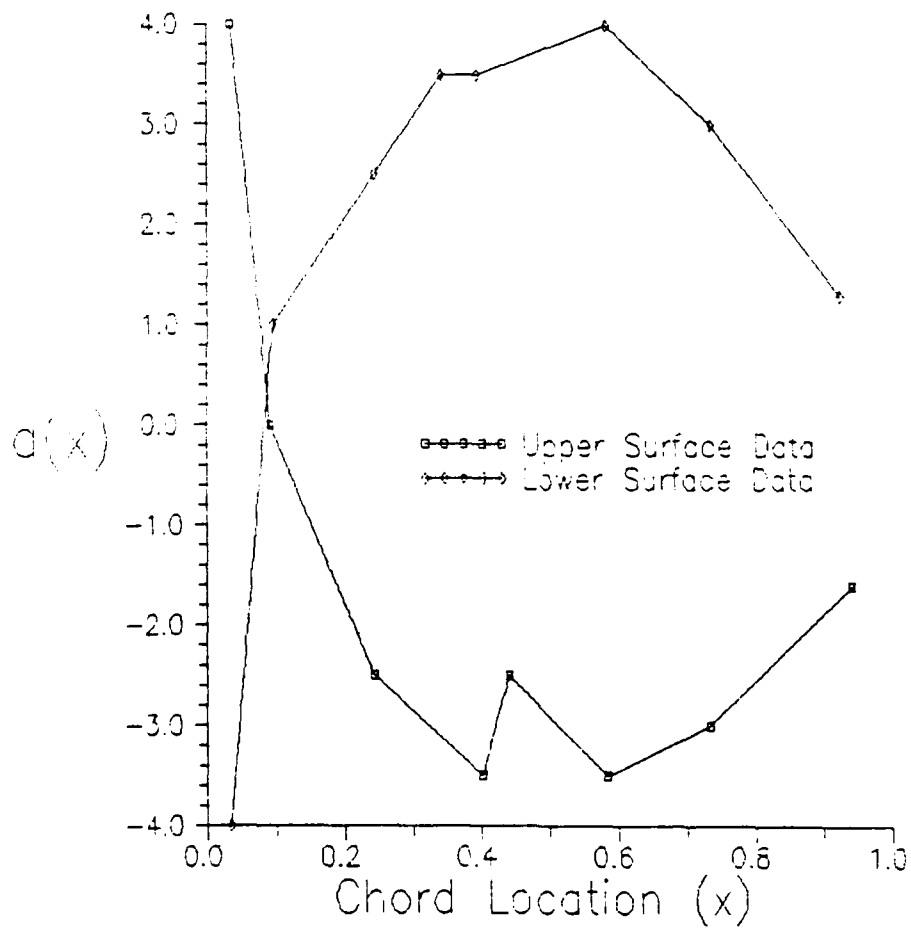


Figure 8. Variation in Phase Lag

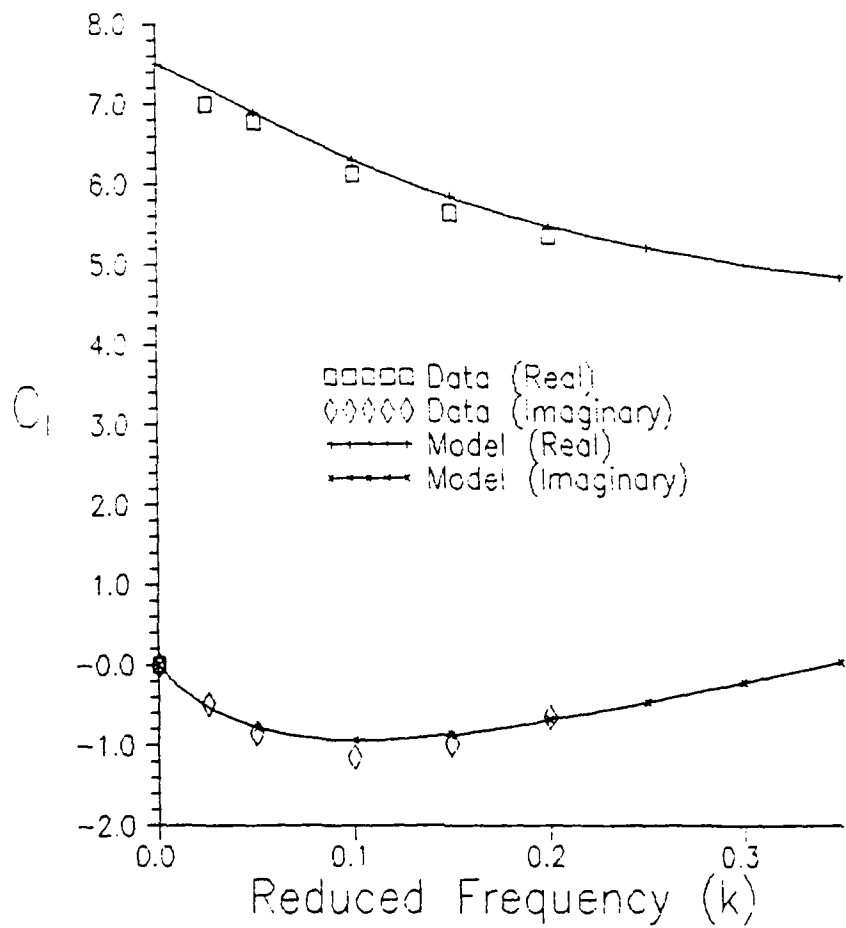


Figure 9. Lift Coefficient Variation

The fractional calculus model of the Theodorsen function serves as a sound foundation for modeling experimental data. It captures the theoretical behavior of the function and so provides a good model of the physical behavior of an airfoil in simple harmonic unsteady flow.

III. Time Domain Functions

One approach to applying Theodorsen's function to more generalized unsteady flow is to find the time domain response of a typical section to a prescribed flow condition. Wagner's function and Küssner's function are common time domain representations of the response of a typical section to unsteady flows. Both are dimensionless scaling functions which modify the lift which would act on a typical section if the flow were "steady" at the new values. As a result of this, both functions approach unity for large arguments as the lift builds to its steady state value.

Wagner's function is the time domain response of the Theodorsen function to a unit step change in circulation. It represents the effect of a sudden change in angle of incidence or vertical gust velocity on unsteady circulatory lift. It may be found by solving the convolution of the time domain transform of Theodorsen's function with the unit step function (3:284).

The convolution which produces Küssner's function is somewhat more complex. Küssner's function is the time domain response of Theodorsen's function to a sharp-edged change in vertical gust velocity as it is entered by a typical section. This results in a convolution of the time domain transform of Theodorsen's function with a travelling wave. Both of these convolutions are performed in the Laplace domain and transformed to provide time domain expressions.

Wagner's Function

Wagner's function, $k_1(\sigma)$, describes the time dependent circulatory lift of an airfoil in incompressible flow resulting from a step change in circulation. As a result, Wagner's function is a convolution of Theodorsen's function with the unit step function. While this approach is conceptually simple, it is not possible to evaluate the exact convolution integral in terms of simple functions.

Wagner's function has been approximated by convolution of small argument expansions of the Bessel functions (17:32-36), and has various polynomial and exponential approximations (8:207). The fractional calculus model of Theodorsen's function, however, leads to a simple and accurate representation of Wagner's function through an inverse Laplace transform. In order to find this approximation of Wagner's function, it is necessary to employ a binomial expansion on the Theodorsen function's fractional calculus model. Equation (10) shows the fractional calculus model written in a familiar form to allow a binomial expansion.

$$\hat{C}(\bar{s}) = \frac{1 + F\bar{s}^B}{1 + 2F\bar{s}^B} = \frac{1}{2} + \frac{1}{4F\bar{s}^B} \left[\frac{1}{1 - \left[\frac{-1}{2F\bar{s}^B} \right]} \right] \quad (10)$$

The binomial expansion leads to a series in the form of equation (11).

$$\hat{C}(\bar{s}) = 1 - \frac{1}{2} \sum_{n=0}^{\infty} \left[\left[\frac{-1}{2F\bar{s}^B} \right]^n \right] \quad (11)$$

Each term in the series representation of $C(\bar{s})/\bar{s}$ in equation (11) has a known inverse Laplace transform, so the convolution integral may be evaluated by multiplication in the Laplace domain. Wagner's function can be defined as $k_1(\sigma) = L^{-1}\{C(\bar{s})/\bar{s}\}$ where $\sigma = tU/b$ is dimensionless time as shown in equation (12). Equation (13) gives the transformed equivalent in the time domain.

$$k_1(\sigma) = L^{-1} \left[\frac{1}{\bar{s}} - \frac{1}{2} \sum_{n=0}^{\infty} \left[\left[\frac{-1}{2F\bar{s}^{\beta+1}} \right]^n \right] \right] \quad (12)$$

$$= u_{-1}(\sigma) - \frac{1}{2} \sum_{n=0}^{\infty} \left[\left[\frac{1}{2F} \right]^n \frac{\sigma^{n\beta}}{\Gamma(1+n\beta)} \right] \quad (13)$$

The series in equation (13) is a special case of a generalized exponential function called the Mittag-Leffler function $E_{\beta}(x)$ (15:102). The definition of the beta order Mittag-Leffler function is given in equation (14)

$$E_{\beta}(x) = \sum_{n=0}^{\infty} \left[\frac{x^n}{\Gamma(1+n\beta)} \right] \quad (14)$$

$$k_1(\sigma) = u_{-1}(\sigma) - \frac{1}{2} E_{\beta} \left[\left[\frac{\sigma}{(2F)^{1/\beta}} \right]^{\beta} \right] \quad (15)$$

Figure 10 shows the Mittag-Leffler (order $\beta=5/6$) approximation to Wagner's function from equation (15) plotted against values calculated by Sears (17:38) using several Bessel function expansion equations. Several equations were necessary to approximate Wagner's function

since the expansions of the Bessel functions Sears used apply only to limited ranges of the argument.

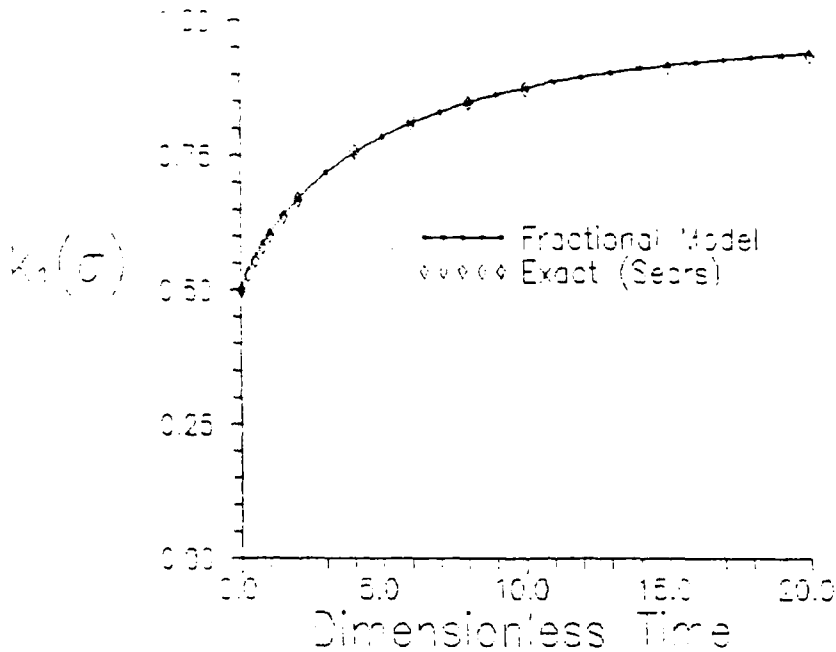


Figure 10. Wagner's Function

Küssner's Function

Küssner's function is more complex than Wagner's. It is a time domain representation of the response of an airfoil section to a change in circulation resulting from a sharp-edged change in vertical gust velocity. It describes the change in circulatory lift on an airfoil in initially steady flow as it penetrates a step change in vertical gust velocity (3:286-289). As with Wagner's function, there is no way to evaluate the exact integral in terms of simple functions. The exact definition of Küssner's function is given in equation (16).

$$k_2(\sigma) = L^{-1}\{e^{-\bar{s}}[(I_0(\bar{s}) - I_1(\bar{s}))C(\bar{s}) + I_1(\bar{s})]\} \quad (16)$$

By introducing the fractional calculus model of the Theodorsen function, this can be rewritten as shown in equation (17). The inverse Laplace transform results in the integral approximation given in equation (18).

$$k_2(\sigma) = L^{-1}\{e^{-\bar{s}}I_0(\bar{s})\hat{C}(\bar{s}) + e^{-\bar{s}}I_1(\bar{s})[1-\hat{C}(\bar{s})]\} \quad (17)$$

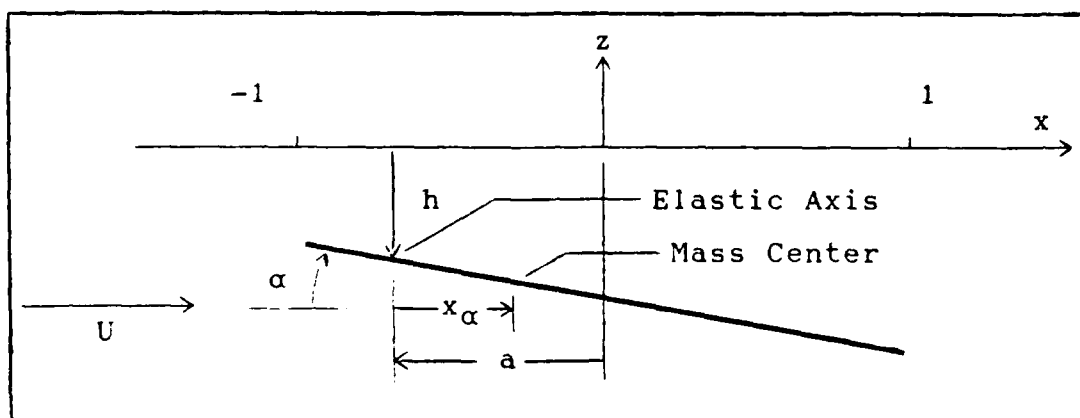
$$k_2(\sigma) = \int_0^\sigma \frac{\frac{d[-\hat{C}(\sigma-\tau)]}{d\sigma} \tau [u_{-1}(\tau) - u_{-1}(\tau-2)]}{\pi[\tau(2-\tau)]^{1/2}} d\tau + \frac{(1-\sigma)[u_{-1}(\sigma) - u_{-1}(\sigma-2)]}{\pi[\sigma(2-\sigma)]^{1/2}} \quad (18)$$

Küssner's function can not be readily simplified from this form. Various other integral forms of this function are available for numerical calculations, but the most common representation used are exponential approximations (3:285-288), (8:344-348).

IV. Flutter Prediction

In order to predict system instability, we need to determine the system's eigenvalues. The eigenvalues can be found by solving the eigenvalue problem for a typical airfoil section. Figure 11 shows a typical airfoil section with its characteristic parameters.

Figure 11. Typical Section Geometry



For a two degree of freedom model of an airfoil, the Laplace domain equations of motion are written in matrix form in equation (19). (7:7-8,165-167)

$$\{[M]s^2 + [K]\}\{x_s\} = [L]\{x_s\}/m_s b^2 \quad (19)$$

Here

$$[M] = \begin{bmatrix} 1 & x_\alpha \\ x_\alpha & r_\alpha^2 \end{bmatrix} \quad [K] = \begin{bmatrix} \omega_h^2 & 0 \\ 0 & r_\alpha^2 \omega_\alpha^2 \end{bmatrix} \quad \{x_s\} = \begin{bmatrix} h_s \\ \alpha_s \end{bmatrix}$$

The mass/inertia matrix [M] contains terms which describe the nondimensionalized structural mass properties of the system. The lift and moment on the section are

coupled by x_α which represents the static imbalance between the center of lift and center of mass for the section. The r_α term is the nondimensionalized section radius of gyration which represents the rotational inertia of the system.

The stiffness matrix $[K]$ contains terms which represent the linear and torsional stiffness associated with the airfoil. These stiffnesses are nondimensionalized to produce the system's natural frequencies ω_α and ω_h .

The lift matrix $[L]$ is more complex. It contains terms which describe both the circulatory and non-circulatory lift acting on an oscillating airfoil. The circulatory terms are described by Theodorsen's function. The non-circulatory terms arise from the "apparent mass" lift which results from the displacement of fluid by the oscillating airfoil (8:446-447).

$$[L] = \{[M_{nc}]s^2 + \{[B_{nc}] + C(\bar{s})[B_c]\}(U/b)s + C(\bar{s})[K_c](U/b)^2\}/\pi\mu \quad (20)$$

Here

$$[M_{nc}] = \begin{bmatrix} -\pi & \pi a \\ \pi a & -\pi(1/8 + a) \end{bmatrix} \quad [B_{nc}] = \begin{bmatrix} 0 & -\pi \\ 0 & \pi(a - \frac{1}{2}) \end{bmatrix}$$

$$[B_c] = 2\pi \begin{bmatrix} -1 & a - \frac{1}{2} \\ a + \frac{1}{2} & (a + \frac{1}{2})(\frac{1}{2} - a) \end{bmatrix} \quad [K_c] = 2\pi \begin{bmatrix} 0 & -1 \\ 0 & (a + \frac{1}{2}) \end{bmatrix}$$

These equations can be reduced to the eigenvalue problem by eliminating the Laplace domain state vector associated with the matrices. This results in what would be a standard eigenvalue problem form if the matrix $[L]$ shown

in equation (21) were not a function of the Laplace variable, \bar{s} .

$$\{[M]s^2 + [K] - [L]/m_s b^2\}\{x_s\} = \{0\} \quad (21)$$

The circulatory lift terms in this equation are described by Theodorsen's function, and the Bessel functions which define Theodorsen's function are transcendental. This means that the equation in exact form cannot be cast as an algebraic eigenvalue problem having constant matrices multiplied by integer powers of the Laplace variable, s .

To overcome this obstacle, Edwards employs an iterative "gradient search" method which begins with an initial guess for each eigenvalue and iterates toward a solution based on a series expansion of the Bessel functions in Theodorsen's function. By using the fractional calculus model of Theodorsen's function, constant coefficient matrices can be separated from the frequency dependent terms in the equation. This produces a set of differential equations of fractional order. It would be possible to use this approach with a polynomial approximation, but the poor accuracy of such functions for complex arguments (as shown previously) would color any results.

Fractional Approach

To construct the fractional order eigenvalue problem, it is convenient to multiply equation (21) by the denominator of the Theodorsen function model as shown in equation (22).

$$(1+2F\bar{s}^{5/6})\{[M]s^2 + [K] - [L]/m_s b^2\}\{x_s\} = \{0\} \quad (22)$$

Note that the Theodorsen function operates on a non-dimensional Laplace variable $s = sb/U$. It is necessary to extract these nondimensionalizing factors from the Theodorsen function to solve the characteristic equation. There is no simple way to factor a constant out of the argument of the exact representation. The fractional calculus model however, allows the dimensional terms to appear explicitly as shown in equation (23).

$$\begin{aligned} & \{[M](s^2+2Fs^{17/6}(U/b)^{-5/6}) \\ & + (1+2Fs^{5/6}(U/b)^{-5/6})\{[K] - [L]/m_s b^2\}\{x_s\} = \{0\} \quad (23) \end{aligned}$$

Using the definitions of these matrices given earlier, this expression can be expanded to the form given in equation (24). (A more complete development of this equation is provided in Appendix B.)

$$\begin{aligned} & \{s^{17/6} 2F(U/b)^{-5/6}\{[M] - [M_{nc}]/\pi\mu\} \\ & + s^2 \{[M] - [M_{nc}]/\pi\mu\} \\ & + s^{11/6} (U/b)F\{2[B_{nc}] + [B_c]\}/\pi\mu \\ & - s (U/b)\{[B_c] + [B_{nc}]\}/\pi\mu \\ & + s^{5/6} F\{2[K](U/b)^{-5/6} - (U/b)^{7/6}[K_c]/\pi\mu\} \\ & + [K] - (U/b)^2[K_c]/\pi\mu\}\{x_s\} = \{0\} \quad (24) \end{aligned}$$

For simplification, the matrices associated with each fractional power of s will be given the distinct notation of equations (25) through (30).

$$[m1] = 2F(U/b)^{-5/6}\{[M] - [M_{nc}]/\pi\mu\} \quad (25)$$

$$[m2] = \{[M] - [M_{nc}]/\pi\mu\} \quad (26)$$

$$[m3] = (U/b)F\{2[B_{nc}] + [B_c]\}/\pi\mu \quad (27)$$

$$[m4] = (U/b)\{[B_c] + [B_{nc}]\}/\pi\mu \quad (28)$$

$$[m5] = F\{2[K](U/b)^{-5/6} - (U/b)^{7/6}[K_c]/\pi\mu\} \quad (29)$$

$$[k] = [K] - (U/b)^2[K_c]/\pi\mu \quad (30)$$

Given these matrix definitions, equation (24) is rewritten

$$\begin{aligned} &\{[m1]s^{17/6} + [m2]s^2 + [m3]s^{11/6} \\ &\quad + [m4]s + [m5]s^{5/6} + [k]\}\{x_s\} = \{0\} \end{aligned} \quad (31)$$

The system eigenvalues and the general solution to equation (31) can now be obtained directly. Fractional order differential equations can be solved numerically and several evaluation techniques, such as the spectrum shift and modified matrix iteration techniques, have been developed for numerical analysis (9:6-18). These methods can be used to solve the eigenvalue problem.

Rather than introduce these techniques, this thesis will present an eigenvalue solution using a simpler algebraic technique. This solution to the fractional order state equation has been published (1:488-489) with an example for 1/2 order fractional powers. The penalty for constructing the equations using this technique is a higher order equation. The solution for the 1/6 order state equation yields a pair of real, symmetric matrices of order

The eigenvalues of the equation in this form can be found using most common matrix manipulation programs without using the specialized solvers mentioned earlier. Appendix C contains a simple MATLAB algorithm implementation of this solution. This solution yields 34 eigenvalues in the Laplace $s^{1/6}$ plane. Only two pairs of these eigenvalues (those on the primary branch) will map into the primary Laplace s plane. These eigenvalues correspond to the pitch and plunge degrees of freedom of the typical section. The remaining eigenvalues fall on other Riemann sheets when mapped under the z^6 transformation from the $s^{1/6}$ plane to the s plane.

Figure 12 shows a typical distribution of eigenvalues in the $s^{1/6}$ plane produced by a MATLAB matrix solution for $U/b=300$. Each primary branch eigenvalue in the $s^{1/6}$ plane can be raised to the sixth power to map it onto the standard Laplace plane. Figure 13 shows the standard Laplace plane with the primary branch eigenvalues from Figure 12 mapped into their proper locations.

The stability of the system is easily determined since the system eigenvalues are known. A complete root-locus plot of the system eigenvalues can be generated by varying the airspeed factor U/b . The flutter speed occurs when one of the system eigenvalues crosses the imaginary axis into the right half s -plane. Divergence occurs when one of a pair of eigenvalues which have reached the negative real axis crosses onto the positive real axis.

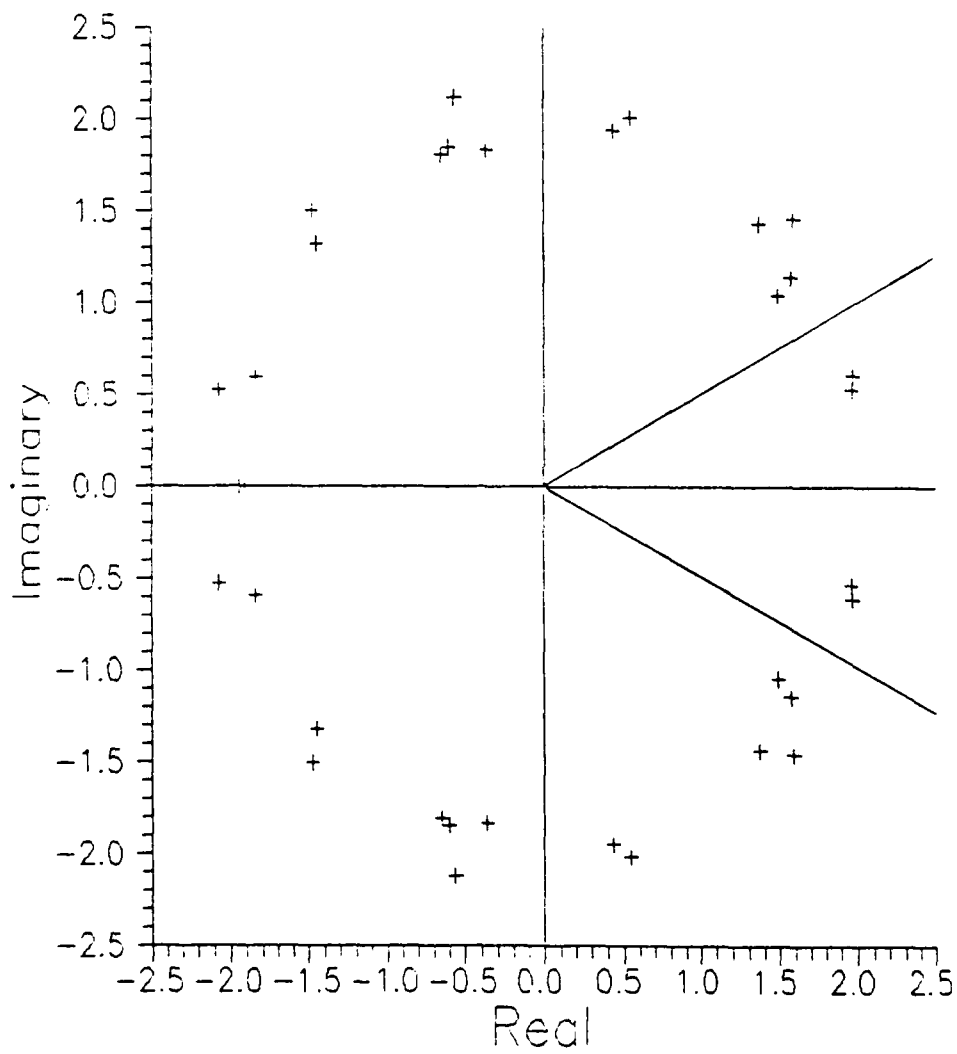


Figure 12. $s^{1/6}$ plane eigenvalues

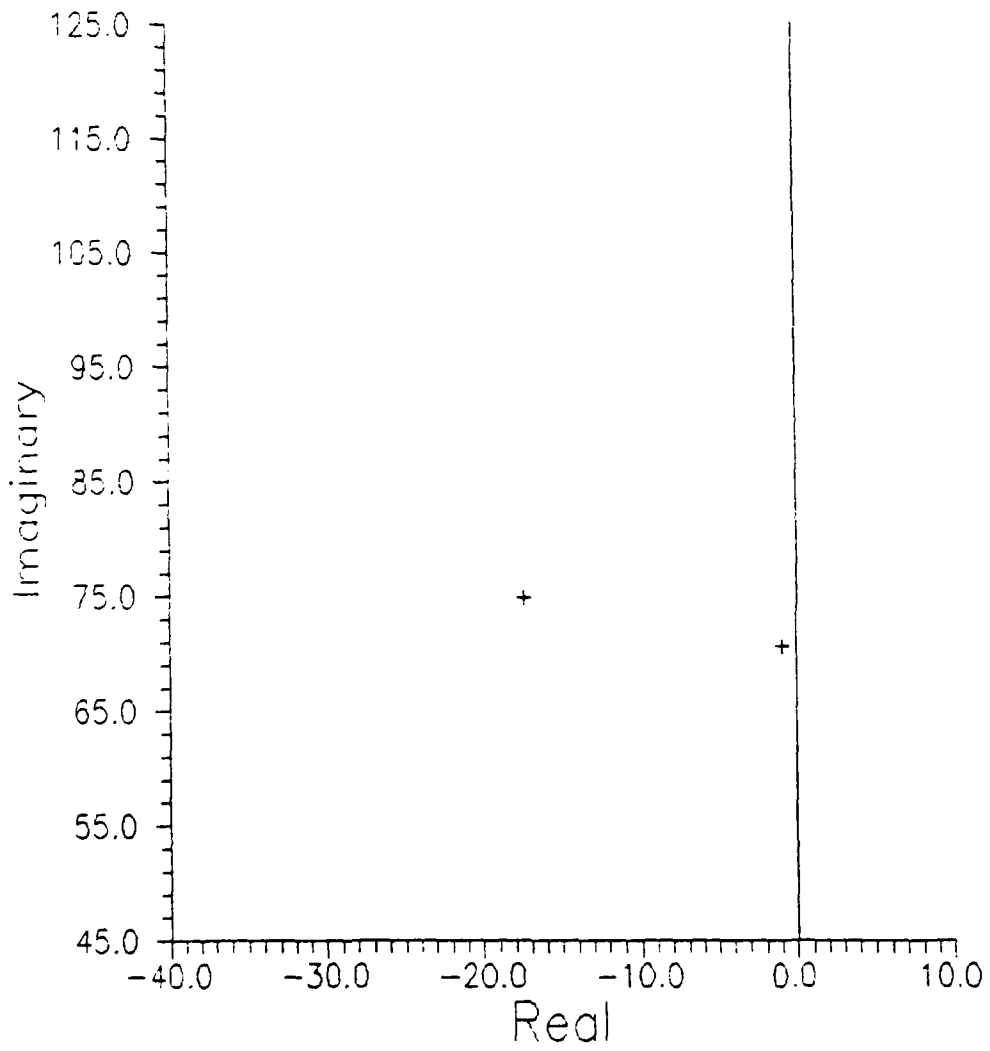


Figure 13. s plane eigenvalues

Comparison With Existing Methods

Few methods exist for determining aeroelastic system stability by actual extraction of system eigenvalues. The value of such methods has been known for some time. Goland and Luke presented an early attempt at finding flutter speed by iterative calculation to find aerodynamic damping (10:389-395). More recently, Edwards has presented a modern gradient search method of iteration for section eigenvalues (7:45-51). In the same paper, he introduces a Padé approximate and augmented states solution for system eigenvalues. This method produces a state equation of higher order and requires considerable manipulation of the original equation to reach a solvable form (7:63-72).

Figure 14 shows the root locus plot generated by Edwards using his iterative solution (7:51). Figure 15 shows the root locus plot generated by the fractional order state equation solution.

The fractional solution models the behavior and magnitude of Edwards' solution quite well. The actual flutter speed of the models varies slightly because Edwards' model includes the effect of an unbalanced trailing edge flap.

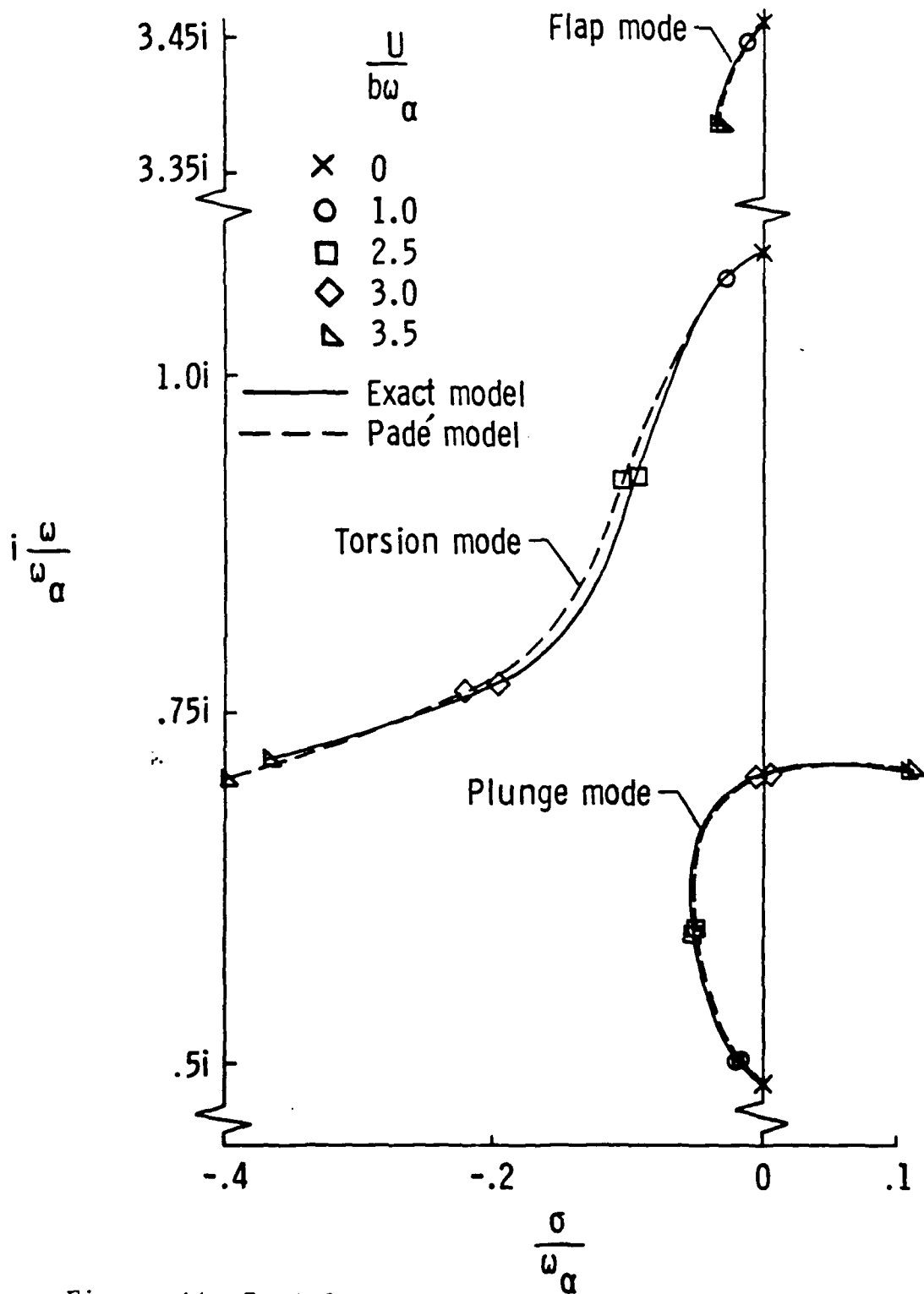


Figure 14. Root Locus

Edwards (7:51)

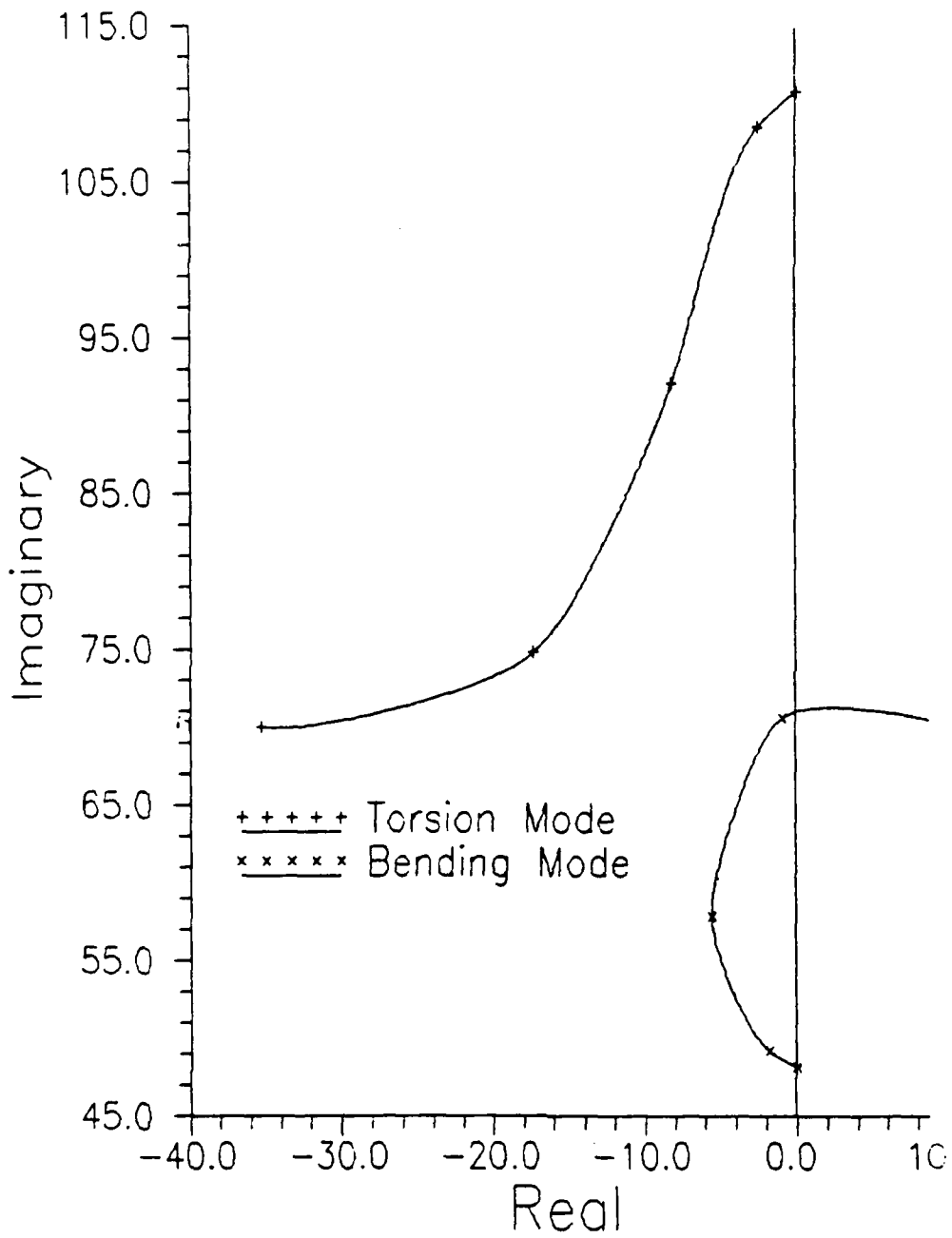


Figure 15. Root Locus
Fractional Method

VI. Summary and Conclusions

The fractional calculus eigenvalue problem formulation has a number of advantages over existing techniques. It provides a graphic and accurate analytic description of system stability, a measure of the rate of approach to instability, and a form ideal for stability and control analysis.

The fractional order state equation method provides several advantages over the series expansion approximations of the Theodorsen function. The fractional calculus model is accurate over many decades of reduced frequency; the series expansions require either large numbers of terms or more than one series to provide accuracy for both large and small arguments. The fractional calculus model captures the complete behavior of the function, but does not produce transcendental characteristic equations. This makes the model easier to manipulate mathematically and allows the nondimensionalizing constants in its argument to be easily factored out. The model has a known inverse transform, so it yields consistent approximations to time domain functions. These advantages over the series approximation to the Theodorsen function allow the development of an equation of motion with constant coefficient matrices.

The fractional order state equation method also provides several advantages over the integer polynomial approximations of the Theodorsen function. The polynomial models can be used to develop equations of motion with constant coefficient matrices, but problems arise. The poor accuracy of polynomial models for fully complex arguments

make it difficult to apply them to decaying unsteady motions. The negative real poles of integer polynomial models make them difficult to apply to divergence instability. These poles must be shifted away from the axis to produce a divergence model in addition to a flutter model. The fractional calculus model avoids this problem since it does not have poles on the principal branch of the s plane.

The fractional calculus model has fewer parameters than any other available approximation. It reproduces the trends of the Theodorsen function with good accuracy for all arguments, and so can be employed in a wide range of unsteady motions.

The advantages of the fractional order state equation model make it an ideal tool for modeling unsteady aeroelasticity. It is a simple concept which can be generalized to more complex models. The necessary equations for including the effects of control surfaces are given by Edwards (7:7-8,165-166). It could be adapted for use in existing models of three-dimensional aeroelastic behavior, such as turbine blade dynamics or helicopter rotor dynamics, which rely on eigenstructure determination.

In summary, the fractional order state equation model has been shown to be an effective tool for aeroelastic analysis. Its form is compatible with existing control theory analysis techniques and will integrate easily with them. It gives a compact, accurate and flexible approximation to the effects of unsteady flow and allows direct solution of the forces on an airfoil.

Appendix A: Complex Pressure Coefficient Data

This appendix compares fractional approximations of unsteady aerodynamic pressures to data on an airfoil (NACA 64A010) oscillating in pitch about 1/4 chord at Mach 0.5 and Reynolds # = 9.9E6 (5:15). The real and imaginary parts of the complex pressure are modeled using equation (8).

$$C_p = A(x)\hat{C}(ik) + d(x)(ik) \quad (8)$$

Data

Model

Upper Surface Complex Pressure Coefficient

Real

Imaginary

$$A(x=.033) = -12$$

$$d(x=.033) = 4$$

-16

-1

Re C
P

Im C
P

4

0

k

0.35

4

0

k

0.35

$$A(x=.091) = -8.2$$

$$d(x=.091) = 0$$

-16

-1

Re C
P

Im C
P

4

0

k

0.35

4

0

k

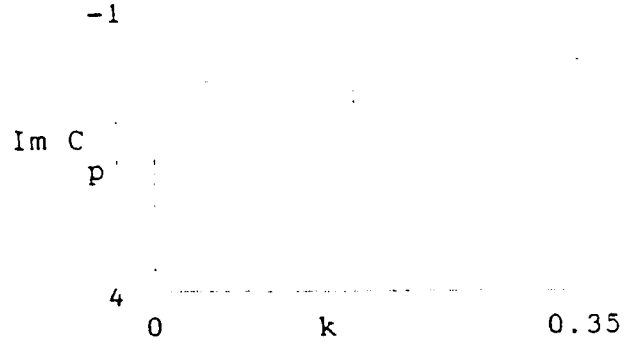
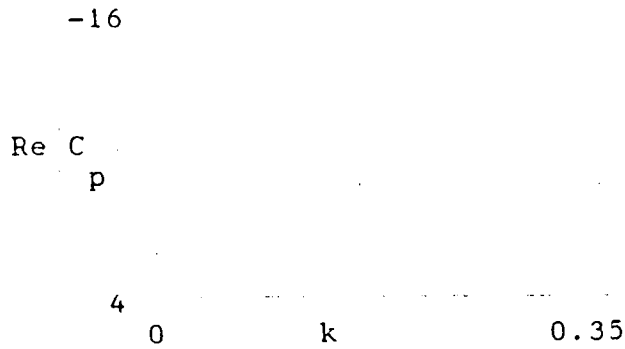
0.35

Upper Surface Complex Pressure Coefficient

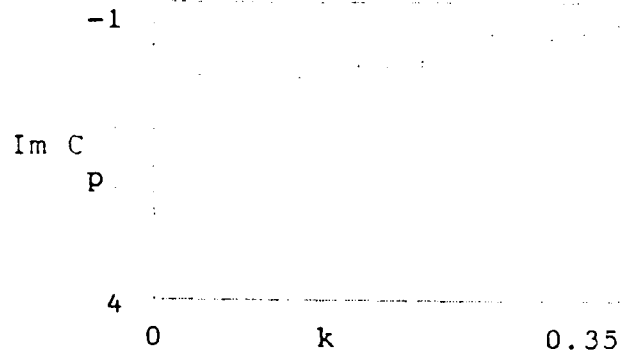
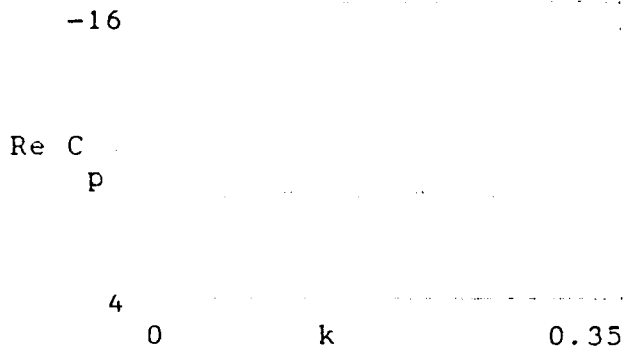
Real

Imaginary

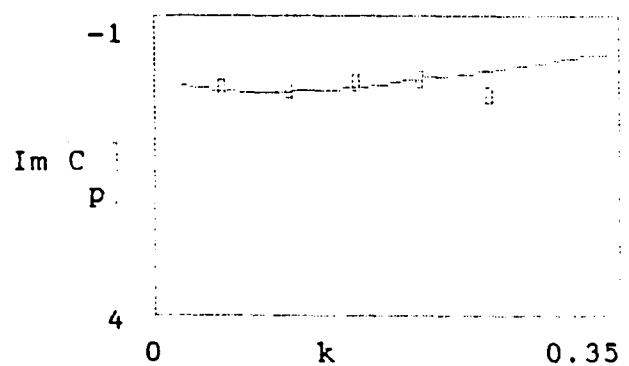
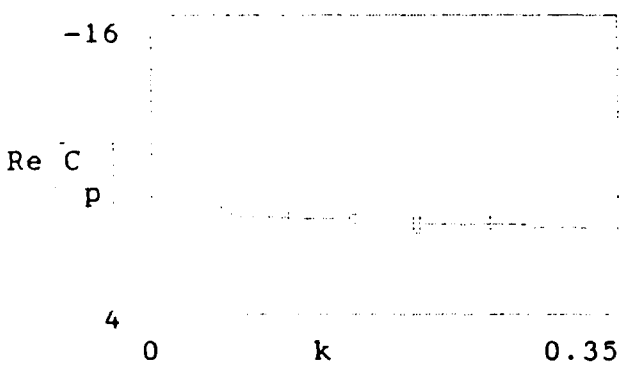
$A(x=.243) = -5.2$
 $d(x=.243) = -2.5$



$A(x=.402) = -3.7$
 $d(x=.402) = -3.5$



$A(x=.440) = -2.9$
 $d(x=.440) = -2.5$



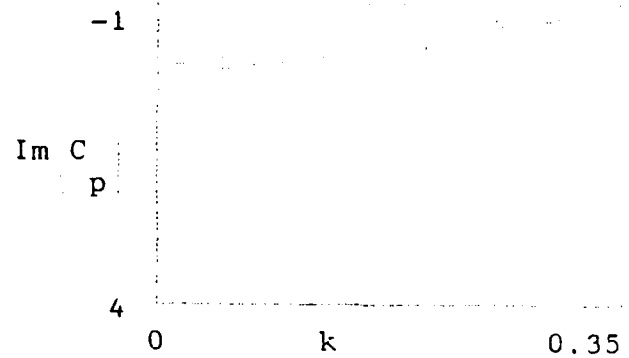
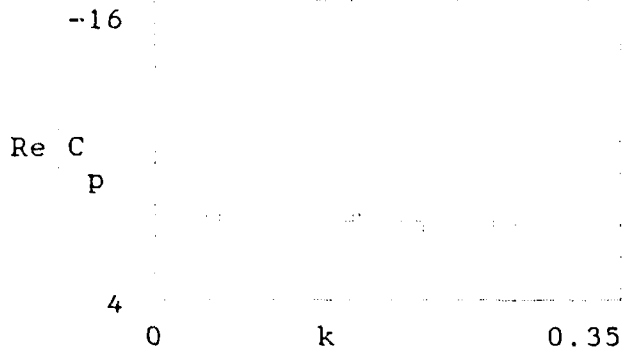
Upper Surface Complex Pressure Coefficient

Real

Imaginary

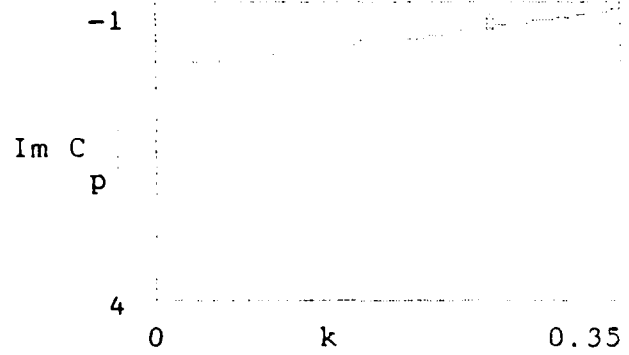
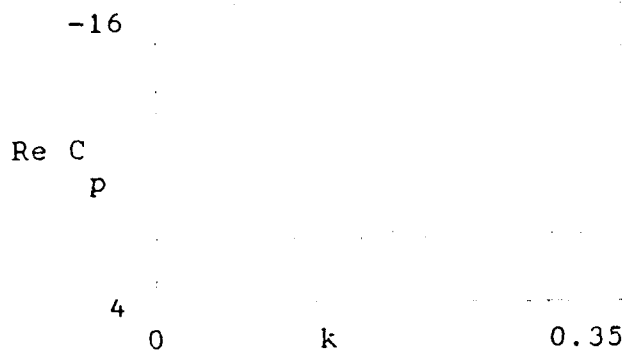
$$A(x=.584) = -1.7$$

$$d(x=.584) = -3.5$$



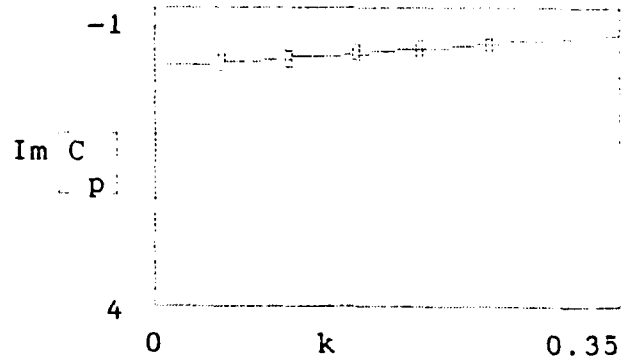
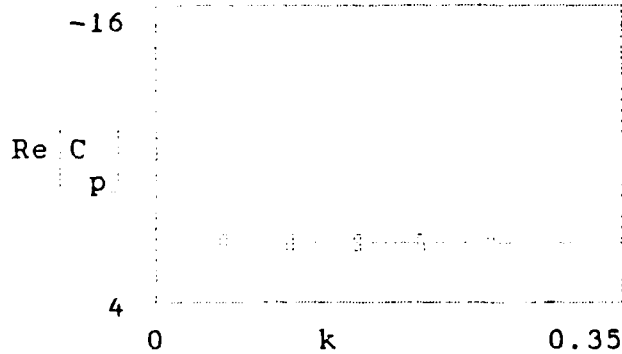
$$A(x=.733) = -1$$

$$d(x=.733) = -3$$



$$A(x=.941) = -.15$$

$$d(x=.941) = -1.6$$

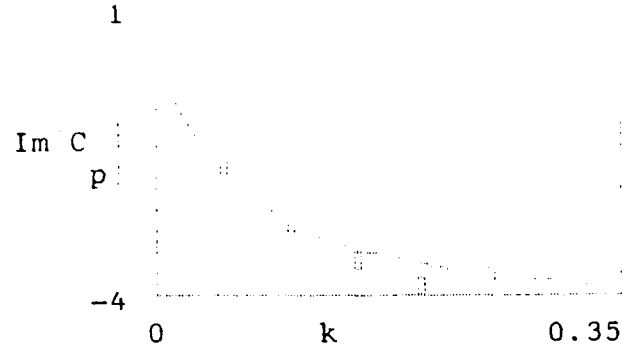
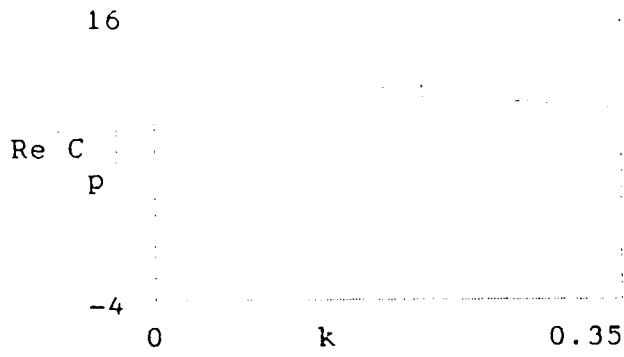


Lower Surface Complex Pressure Coefficient

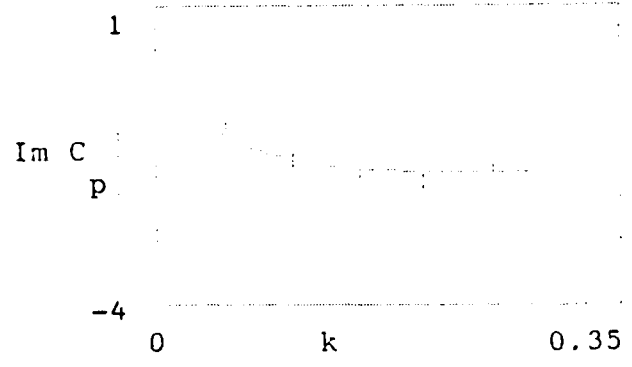
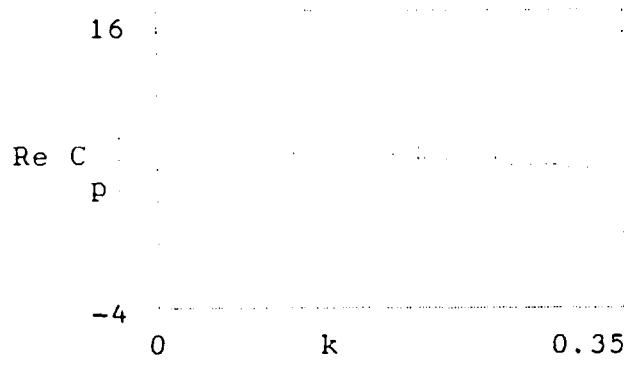
Real

Imaginary

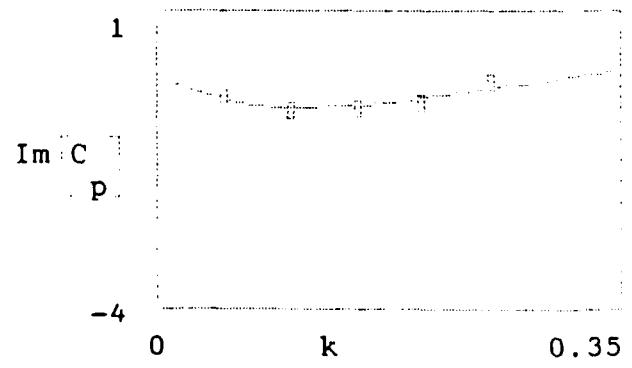
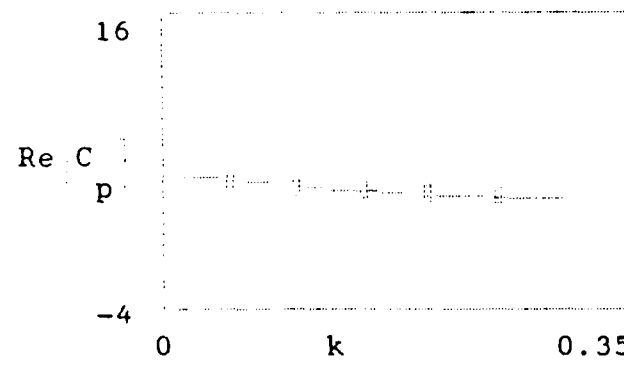
$A(x=.034) = 13.5$
 $d(x=.034) = -4.5$



$A(x=.094) = 8.3$
 $d(x=.094) = -1$



$A(x=.243) = 5$
 $d(x=.243) = 2.5$

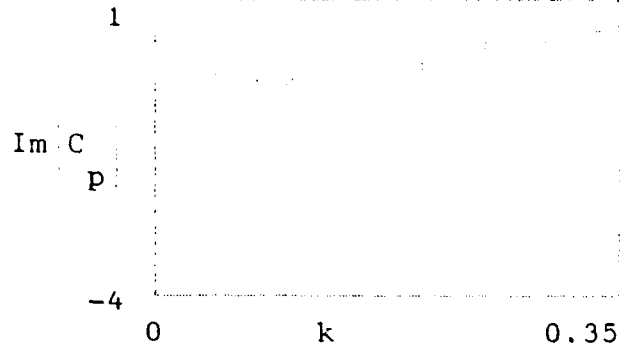
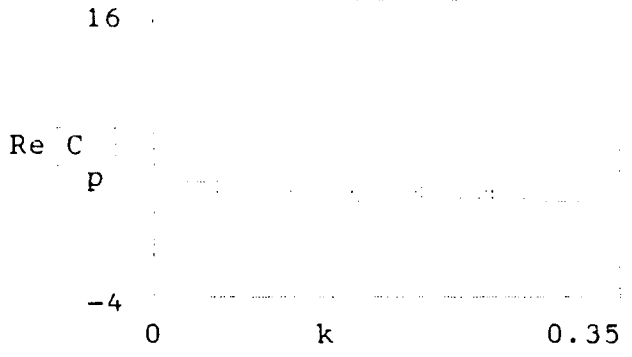


Lower Surface Complex Pressure Coefficient

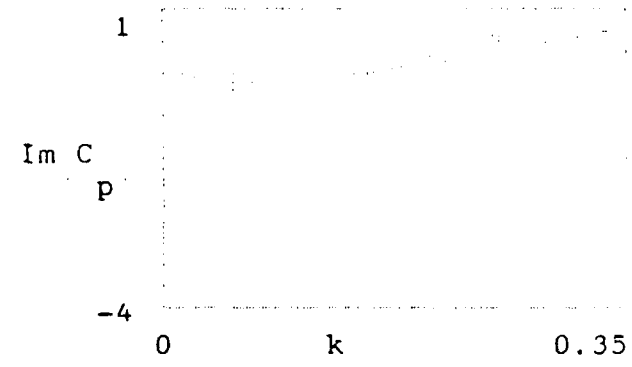
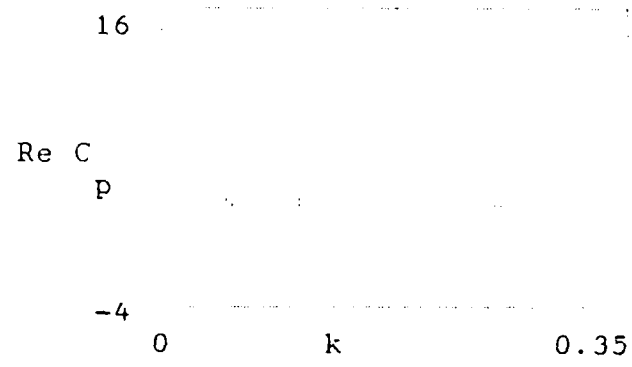
Real

Imaginary

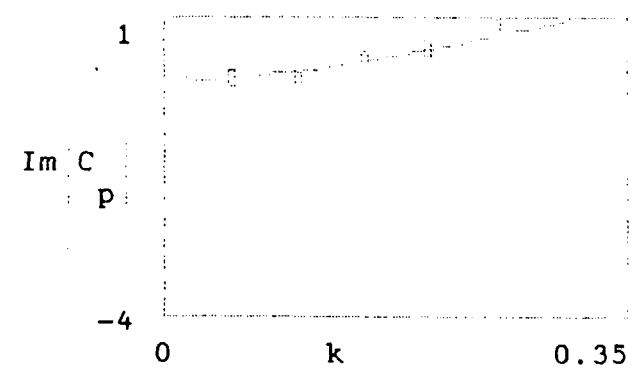
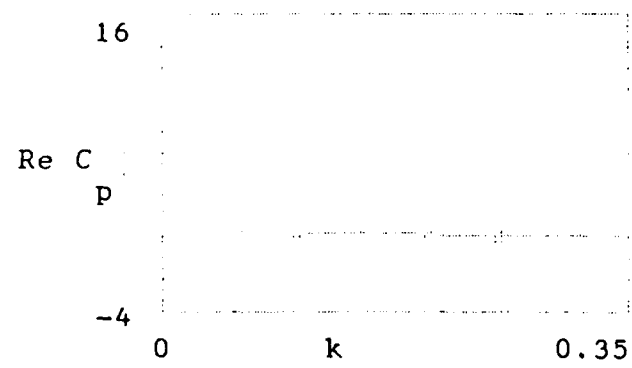
$A(x=.341) = 3.9$
 $d(x=.341) = 3.5$



$A(x=.394) = 3.2$
 $d(x=.394) = 3.5$



$A(x=.582) = 1.7$
 $d(x=.582) = 4$



Lower Surface Complex Pressure Coefficient

Real

Imaginary

$$A(x=.733) = .9$$
$$d(x=.733) = 3$$

16

1

Re C
P

-4

0

k

0.35

Im C

P

-4

0

k

0.35

$$A(x=.923) = .15$$
$$d(x=.923) = 1.3$$

16

1

Re C
P

-4

0

k

0.35

Im C

P

-4

0

k

0.35

Appendix B: Fractional Order State Equation

Given the system eigenvalue problem (B.1), we must first multiply all terms by the denominator of the Theodorsen function model $(1+2F\bar{s}^{5/6})$. This produces equation (B.2).

$$\{[M]s^2 + [K] - [L]/(m_s b^2)\}\{x_s\} = \{0\} \quad (B.1)$$

$$\begin{aligned} \{ [M] (s^2 + 2F\bar{s}^{5/6}) \\ + (1+2F\bar{s}^{5/6})\{[K] - [L]/(m_s b^2)\} \}\{x_s\} = \{0\} \end{aligned} \quad (B.2)$$

Since only the terms in $[L]$ contain $C(s)$ as shown in equation (B.3), we can reform equation (B.2) as (B.4).

$$\begin{aligned} [L] = \{ [M_{nc}]s^2 + \{ [B_{nc}] + C(s)[B_c] \}(U/b)s \\ + C(s)[K_c](U/b)^2 \} / \pi\mu \end{aligned} \quad (B.3)$$

$$\begin{aligned} \{ [M] (s^2 + 2F\bar{s}^{5/6}) + (1+2F\bar{s}^{5/6})[K] \\ - (1+2F\bar{s}^{5/6})\{ [M_{nc}]s^2 + [B_{nc}]s \} / (\pi\mu) \} \\ + (1+F\bar{s}^{5/6})\{ [B_c]s + [K_c] \} / (\pi\mu) \}\{x_s\} = \{0\} \end{aligned} \quad (B.4)$$

The nondimensionalizing constants in $s = sb/U$ can be factored out to provide a consistent function of a single Laplace variable s . This results in equation (B.5)

$$\begin{aligned} \{ [M] (s^2 + 2F\bar{s}^{5/6}(b/U)^{5/6}s^{5/6}) + (1+2F(b/U)^{5/6}\bar{s}^{5/6})[K] \\ - (1+2F(b/U)^{5/6}\bar{s}^{5/6})\{ [M_{nc}]s^2 + [B_{nc}]s \} / (\pi\mu) \} \\ + (1+F(b/U)^{5/6}\bar{s}^{5/6})\{ [B_c]s + [K_c] \} \}\{x_s\} = \{0\} \end{aligned} \quad (B.5)$$

Carrying out the multiplication and grouping like order terms reduces the equation to constant matrices and fractional powers of s as shown in equation (B.6).

$$\begin{aligned}
 & \{ s^{17/6} 2F(U/b)^{-5/6} \{ [M] - [M_{nc}] / \pi\mu \} \\
 & + s^2 \{ [M] - [M_{nc}] / \pi\mu \} \\
 & + s^{11/6} (U/b) F \{ 2[B_{nc}] + [B_c] \} / \pi\mu \\
 & - s(U/b) \{ [B_c] + [B_{nc}] \} / \pi\mu \\
 & + s^{5/6} F \{ 2[K] (U/b)^{-5/6} - (U/b)^{7/6} [K_c] / \pi\mu \} \\
 & + [K] - (U/b)^2 [K_c] / \pi\mu \} \{ x_s \} = \{ 0 \} \qquad (B.6)
 \end{aligned}$$

In this form, the state equation can be solved directly using the spectrum shift or modified matrix iteration techniques or by the matrix expansion method (1:488-489). The "pseudomass" and "pseudostiffness" matrices generated by the matrix expansion method are given in equation (32). Appendix C is a MATLAB routine for solution using this method.

Appendix C: MATLAB Matrix Construction and Solution

```

% Input routine for development of Pseudomass and
% Pseudostiffness matrices

mu=input('Enter mass ratio mu ')
xa=input('Enter x-alpha ')
a=input('Enter cg-rotation axis measure a ')
ra2=input('Enter r sub alpha squared ')
wh=input('Enter omega sub h ')
wa=input('Enter omega sub alpha ')
Ub=input('Enter nondimensional velocity U/b ')

% Pseudomass and pseudostiffness matrix generation

F=2.19;           %Theodorsen function coefficient 'F'
alpha=5/6;       % C(s) nondimensionalizing exponent

A=[1+1/mu xa-a/mu;xa-a/mu ra2+(.125+a^2)/mu];
B=[0 -pi;0 pi*(a-.5)];
C=2*pi*[-1 a-.5;a+.5 (a+.5)*(.5-a)];
D=[wh^2 0;0 wa^2*ra2];
E=2*pi*[0 -1;0 a+.5];

m1=2*F*Ub^(-alpha)*A;           %17/6 term
m2=A;                           %12/6 term (s*s)
m3=-(Ub^(1-alpha)/(pi*mu))*(2*F*B+F*C); %11/6 term
m4=-(Ub/(pi*mu))*(B+C);        % 6/6 term (s)
m5=2*F*Ub^(-alpha)*D-(F*Ub^(2-alpha)/(pi*mu))*E;% 5/6 term
k=D-Ub^2/(pi*mu)*E;           % 0/6 term (1)

% Construction of Pseudomass and Pseudostiffness matrices
b1=zeros(8);
bm=zeros(2);
em1=[bm bm bm m1;bm bm m1 bm;bm m1 bm bm;m1 bm bm bm];
em2=[bm bm bm bm;bm bm bm m2;bm bm m2 m3;bm m2 m3 bm];
em3=[m2 m3 bm bm;m3 bm bm bm;bm bm bm bm;bm bm bm m4];
em4=[bm bm m4 m5;bm m4 m5 bm;m4 m5 bm bm;m5 bm bm bm];

H=[b1 b1 b1 em1;b1 b1 em1 em2;b1 em1 em2 em3;em1 em2 em3 em4];
bn=zeros(32,2);

M=[bn H;m1 bm bm bm bm m2 m3 bm bm bm bm m4 m5 bm bm bm bm];
K=[-H bn;bm bm k];
clear m1 m2 m3 m4 m5 em1 em2 em3 em4 b1 bm bn k H

%MATLAB eigenvalue solver

v=eig(-inv(M)*K)

```

Bibliography

1. Bagley, R.L. and Calico, R.A. "The Fractional Order State Equations for the Control of Viscoelastically Damped Structures," AIAA Paper No. 89-1213, 1989.
2. Bagley, Ronald L. and Torvik, Peter J. "Fractional Calculus-A Different Approach to the Analysis of Viscoelastically Damped Structures". AIAA Journal, 21: 741-748 (May, 1983).
3. Bisplinghoff, Raymond L. et al. Aeroelasticity. Addison Wesley, Mass. 1955.
4. Bisplinghoff, Raymond L. and Ashley, Holt Principles of Aeroelasticity. John Wiley and Sons Inc. New York, NY. 1962.
5. Davis, Sanford S. and Malcolm, Gerald M. Experimental Unsteady Aerodynamics of Conventional and Supercritical Airfoils. NASA Technical Memorandum 81221.
6. Dowell, Earl H. A Modern Course in Aeroelasticity. Sijthoff & Noordhoff, Alphen aan den Rijn, The Netherlands. 1978.
7. Edwards, John W. Unsteady Aerodynamic Modeling and Active Aeroelastic Control. PhD dissertation. Stanford University, Stanford CA, 1977.
8. Fung, Y.C. An Introduction To The Theory Of Aeroelasticity. John Wiley and Sons Inc. New York, NY. 1955.
9. Gaudreault, M.L.D. and Bagley, R.L. "Improved Solution Techniques for the Eigenstructure of Fractional Order Systems," AIAA Paper No. 89-1394, 1989.
10. Goland, Martin and Luke, Yudell L. "A Study of the Bending-Torsion Aeroelastic Modes for Aircraft Wings". Journal of the Aeronautical Sciences, 16: 389-396 (July, 1949).
11. Jones, R.T. "The Unsteady Lift of a Wing of Finite Aspect Ratio". Twenty-Sixth Annual Report of the National Advisory Committee for Aeronautics, 1940. Technical Report #681:31-38. USGPO Wash DC 1941
12. Jones, W.P. "The Generalized Theodorsen Function". Journal of the Aeronautical Sciences, 19: 213 (March, 1952).
13. Laitone, E.V. "Theodorsen Circulation Function for Generalized Motion". Journal of the Aeronautical Sciences, 19: 211-213 (March, 1952).

14. Luke, Y.L. and Dengler, M.A. "Tables of the Theodorsen Circulation Function for Generalized Motion". Journal of the Aeronautical Sciences, 18: 478-483 (July, 1951).
15. Mittag-Leffler, G. "Sur La Représentation Analytique D'une Branch Uniforme D'une Fonction Monogine". Acta Mathematica, 29:101 (1905)
16. MSC/NASTRAN User's Manual, Section 1.11:6-7
17. Sears, William R. Collected Papers of W. R. Sears Through 1973. Cornell University Press (1973).
18. Van de Vooren, A.I. "Generalization of the Theodorsen Function to Stable Oscillations". Journal of the Aeronautical Sciences, 19: 209-211 (March, 1952).

Vita

Captain David V. Swinney [REDACTED]

[REDACTED] He graduated from high school in Choctaw, Oklahoma, in 1980 and attended Oklahoma State University, from which he received the degree of Bachelor of Science in Mechanical Engineering in May 1984. Upon graduation, he received a commission in the USAF through the ROTC program. He entered active duty at Tinker AFB, Oklahoma where he served as a project engineer for the E-4 NEACP, E-3 AWACS and C-18 ARIA aircraft until he entered the School of Engineering, Air Force Institute of Technology, in June, 1988.

REPORT DOCUMENTATION PAGE

Form Approved
OMB No. 0704-0188

1a. REPORT SECURITY CLASSIFICATION Unclassified		1b. RESTRICTIVE MARKINGS	
2a. SECURITY CLASSIFICATION AUTHORITY		3. DISTRIBUTION / AVAILABILITY OF REPORT Approved for public release; distribution unlimited.	
2b. DECLASSIFICATION / DOWNGRADING SCHEDULE		4. PERFORMING ORGANIZATION REPORT NUMBER(S) AFIT/GA/ENY/89D-5	
4. PERFORMING ORGANIZATION REPORT NUMBER(S)		5. MONITORING ORGANIZATION REPORT NUMBER(S)	
6a. NAME OF PERFORMING ORGANIZATION School of Engineering	6b. OFFICE SYMBOL (If applicable) AFIT/ENY	7a. NAME OF MONITORING ORGANIZATION	
6c. ADDRESS (City, State, and ZIP Code) Air Force Institute of Technology Wright-Patterson AFB, OH 45433-6583		7b. ADDRESS (City, State, and ZIP Code)	
8a. NAME OF FUNDING / SPONSORING ORGANIZATION Turbine Engine Division Components Branch	8b. OFFICE SYMBOL (If applicable) WFDC/PCTC	9. PROCUREMENT INSTRUMENT IDENTIFICATION NUMBER	
8c. ADDRESS (City, State, and ZIP Code)		10. SOURCE OF FUNDING NUMBERS	
		PROGRAM ELEMENT NO.	PROJECT NO.
		TASK NO.	WORK UNIT ACCESSION NO.

11. TITLE (Include Security Classification)
A FRACTIONAL CALCULUS MODEL OF AEROELASTICITY

12. PERSONAL AUTHOR(S)
David Vincent Swinney, P.S., Captain, USAF

13a. TYPE OF REPORT MS Thesis	13b. TIME COVERED FROM _____ TO _____	14. DATE OF REPORT (Year, Month, Day) 1989 December	15. PAGE COUNT 58
---	--	---	-----------------------------

16. SUPPLEMENTARY NOTATION

17. COSATI CODES			18. SUBJECT TERMS (Continue on reverse if necessary and identify by block number) Aeroelasticity, Control theory fractional derivative, fractional calculus. Thesis (S1)
FIELD	GROUP	SUB-GROUP	
20	04		
12	09		

19. ABSTRACT (Continue on reverse if necessary and identify by block number)

Thesis Advisor: **Ronald L. Bagley, LtCol, USAF**
Deputy Department Head
Department of Aeronautics/Astronautics

This thesis introduces a new model of aeroelastic behavior. It simplifies the unsteady aerodynamic force expressions for a flat plate by employing fractional order time derivatives to create a compact fractional order polynomial model of Theodorsen's function. This model is used to reduce the system equations of motion to a single fractional derivative eigenvalue problem. The eigenvalue problem is solved at increasing airspeeds to produce a root locus plot of system stability using airspeed as a "gain". This method is shown to yield accurate system instability speeds. *Kenneth*

20. DISTRIBUTION / AVAILABILITY OF ABSTRACT <input checked="" type="checkbox"/> UNCLASSIFIED/UNLIMITED <input type="checkbox"/> SAME AS RPT. <input type="checkbox"/> DTIC USERS		21. ABSTRACT SECURITY CLASSIFICATION Unclassified	
22a. NAME OF RESPONSIBLE INDIVIDUAL Ronald L. Bagley, LtCol, USAF		22b. TELEPHONE (Include Area Code) (512) 255-3517	22c. OFFICE SYMBOL ENY